



1 Evidence of high N₂ fixation rates in productive waters of the 2 temperate Northeast Atlantic

3
4 Debany Fonseca-Batista^{1,2}, Xuefeng Li^{1,3}, Virginie Riou⁴, Valérie Michotey⁴, Florian Deman¹,
5 François Fripiat⁵, Sophie Guasco⁴, Natacha Brion¹, Nolwenn Lemaitre^{1,6,7}, Manon Tonnard^{6,8},
6 Morgane Gallinari⁶, Hélène Planquette⁶, Frédéric Planchon⁶, Géraldine Sarthou⁶, Marc Elskens¹, Lei
7 Chou³, Frank Dehairs¹

8
9 ¹ Analytical, Environmental and Geo-Chemistry, Earth System Sciences Research Group, Vrije Universiteit Brussel,
10 1050 Brussels, Belgium

11 ² Department of Biology, Dalhousie University, Halifax, Nova Scotia, Canada B3H 4R2

12 ³ Service de Biogéochimie et Modélisation du Système Terre - Océanographie Chimique et Géochimie des Eaux,
13 Université Libre de Bruxelles, 1050 Brussels, Belgium

14 ⁴ Aix-Marseille Université, Mediterranean Institute of Oceanography (MIO), UM 110 CNRS/INSU, IRD, 13288
15 Marseille, France

16 ⁵ Max Planck Institute for Chemistry, Climate Geochemistry Department, 55128 Mainz, Germany

17 ⁶ Laboratoire des sciences de l'Environnement MARIN – CNRS UMR 6539 – Institut Universitaire Européen de la Mer,
18 29280 Plouzané, France

19 ⁷ Department of Earth Sciences, Institute of Geochemistry and Petrology, ETH-Zürich, 8092 Zürich, Switzerland

20 ⁸ Institute for Marine and Antarctic Studies, University of Tasmania, Hobart, TAS 7001, Australia

21

22 *Correspondence to:* Debany Fonseca P. Batista (dbatista8@hotmail.com)

23 **Abstract.** Diazotrophic activity and primary production (PP) were investigated along two transects (Belgica BG2014/14
24 and GEOVIDE cruises) off the western Iberian Margin and the Bay of Biscay (38.8–46.5° N; 8.0–19.7° W) in May 2014
25 close to the end of the spring bloom. We report substantial N₂ fixation activities, reaching up to 65 nmol N L⁻¹ d⁻¹ and
26 1533 μmol N m⁻² d⁻¹ close to the Iberian Margin between 38.8° N and 40.7° N. Similar figures in the basin have only
27 been reported in the temperate and tropical western North Atlantic waters with coastal, shelf or mesohaline
28 characteristics, as opposed to the mostly open ocean conditions studied here. In agreement with previous studies, the
29 qualitative assessment of *nifH* gene diversity (encoding the nitrogenase enzyme that fixes N₂) suggested a predominance
30 of heterotrophic diazotrophs, and the absence of filamentous cyanobacteria. At the sites where N₂ fixation activity was
31 highest sequences affiliated to UCYN-A1, obligate symbiont of eukaryotic prymnesiophyte algae, were recovered. The
32 remaining phylotypes were non-cyanobacterial diazotrophs, known to live in association with suspended particles and
33 zooplankton (i.e., Bacteroidetes, Firmicutes and Proteobacteria). Outside the area of exceptional activity, N₂ fixation in
34 the open ocean and at shelf-influenced sites was also relatively high, ranging from 81 to 384 μmol N m⁻² d⁻¹, but was
35 undetectable in the central Bay of Biscay. We propose that the unexpectedly high heterotrophic N₂ fixation activity
36 recorded at the time of our study was sustained by the availability of phytoplankton derived organic matter (dissolved
37 and/or particulate) resulting from the ongoing to post spring bloom. We pose that this organic material not only sustained
38 bacterial production, but also provided sufficient nutrients essential for the nitrogenase activity (e.g., phosphorus).
39 Dissolved Fe was supplied through atmospheric dust deposition during the month preceding our study and through
40 advection of surface waters from the subtropical region and the shelf area. Our findings stress the need for a more



41 detailed monitoring of the spatial and temporal distribution of oceanic N₂ fixation in productive waters of the temperate
42 North Atlantic to better constrain the basin-scale nitrogen input to the ocean inventory.

43

44 **1 Introduction**

45 Dinitrogen (N₂) fixation is the major pathway of nitrogen (N) input to the global ocean and thereby contributes to
46 sustaining oceanic primary productivity (Falkowski, 1997). The conversion by N₂-fixing micro-organisms (diazotrophs)
47 of dissolved N₂ gas into bioavailable nitrogen also contributes to euphotic layer new production and as such, to the
48 sequestration of atmospheric carbon dioxide into the deep ocean (Gruber, 2008). Estimating the overall contribution of N₂
49 fixation to carbon sequestration in the ocean requires an assessment of the global marine N₂ fixation which is to date a
50 matter of debate (Luo et al., 2012).

51 In tropical and subtropical regions, surface waters characterized by warm, stratified and depleted dissolved inorganic
52 nitrogen (DIN) conditions, are assumed to give a competitive advantage to diazotrophs over other phytoplankton since
53 only they can draw N from the unlimited dissolved N₂ pool for their biosynthesis. The filamentous cyanobacterium
54 *Trichodesmium*, long considered as the most active diazotroph in the global ocean, has mostly been reported from
55 oligotrophic tropical and subtropical regions of the ocean (Dore et al., 2002; Capone et al., 2005; Montoya et al., 2007;
56 Needoba et al., 2007; Moore et al., 2009; Fernández et al., 2010; Snow et al., 2015), thought to represent the optimal
57 environment for its growth and N₂-fixing activity (Capone, 1997; Breitbarth et al., 2007). As such, past estimates of
58 global annual N₂ fixation were mainly based on information gathered from tropical and subtropical regions (Luo et al.,
59 2012). However, it was recently suggested that *Trichodesmium* might also be abundant in temperate waters of the
60 Atlantic (Benavides and Voss, 2015; Rivero-Calle et al., 2016) and Pacific Oceans (Shiozaki et al., 2015), even though
61 these higher latitude areas have been poorly explored for diazotrophic activity. Studies using genetic approaches targeting
62 genes encoding the nitrogenase enzyme that fixes N₂ (e.g. *nifH*), have shown the existence and importance of other
63 diazotrophic organisms which apparently occupy broader ecological niches (Sohm et al., 2011; Zehr, 2011). Small
64 diazotrophs such as unicellular diazotrophic cyanobacteria (UCYN classified in groups A, B and C) and non-
65 cyanobacterial diazotrophs, mostly heterotrophic bacteria (e.g. Alpha and Gammaproteobacteria), have been observed
66 over a wide depth range and latitudinal scale, thus spanning a broad range of temperatures (Langlois et al., 2005, 2008;
67 Krupke et al., 2014; Cabello et al., 2015).

68 In the Northeast Atlantic, the large input of Saharan iron-rich dust alleviating dissolved iron (dFe) limitation of the
69 nitrogenase activity (Fe being a co-factor of the N₂-fixing enzyme) (Raven, 1988; Howard and Rees, 1996), and the
70 upwelling of subsurface waters with low DIN (dissolved inorganic nitrogen) to phosphate ratios (Deutsch et al., 2007;
71 Moore et al., 2009), make this region highly favorable for N₂ fixation activity. In fact, the tropical and subtropical eastern
72 North Atlantic waters have been reported to harbor a particularly diverse diazotrophic community relative to the western
73 border and other basins (Langlois et al., 2008; Zehr, 2011; Ratten et al., 2015). The temperate eastern North Atlantic has
74 even been observed to be a worldwide hotspot of prymnesiophyte-UCYN-A symbiotic associations (Cabello et al., 2015).
75 The discovery of a methodological bias associated to the commonly used ¹⁵N₂ bubble-addition technique (Mohr et al.,
76 2010), and the presence of an abundant diazotrophic community in high latitude regions actively fixing N₂ (Needoba et
77 al., 2007; Rees et al., 2009; Blais et al., 2012; Mulholland et al., 2012; Shiozaki et al., 2015) indicate that more efforts are



78 needed to better constrain oceanic N₂ fixation and diazotrophic diversity. Earlier studies in the Iberian Basin investigated
79 the diazotrophic activity either during stratified water column conditions of boreal summer and autumn (Moore et al.,
80 2009; Benavides et al., 2011; Snow et al., 2015; Fonseca-Batista et al., 2017) or during winter convection period
81 (Rijkenberg et al., 2011; Agawin et al., 2014). In the present work, we provide evidence for the significance of N₂
82 fixation, based on the ¹⁵N₂ dissolution method and examine the *nifH* diversity in the Iberian Basin under ongoing and post
83 spring bloom conditions.

84

85 2 Material and Methods

86 Field experiments were conducted during two nearly simultaneous cruises in May 2014. The Belgica BG2014/14 cruise
87 (21–30 May 2014, R/V Belgica), investigated the Bay of Biscay and the western Iberian Margin. In parallel, the
88 GEOVIDE expedition in the framework of the international GEOTRACES program (GA01 section, May 16 to June 29
89 2014, R/V “Pourquoi pas?”) sailed from Portugal shelf area towards Greenland and ended in Newfoundland, Canada
90 (<http://dx.doi.org/10.17600/14000200>). For the latter expedition, only stations within the Iberian Basin investigated for N₂
91 fixation activity (stations Geo-1, 2, 13 and 21) are considered in this paper and the measurements are compared with
92 those conducted at the six sites studied during the BG2014/14 cruise (stations Bel-3, 5, 7, 9, 11 and 13; Figure 1).

93

94 2.1 Environmental conditions

95 Temperature, salinity and photosynthetically active radiation (PAR) profiles were determined using a conductivity-
96 temperature-depth sensor (SBE 09 and SBE 911+, during the BG2014/14 and GEOVIDE cruises, respectively) fitted on a
97 rosette equipped with either 12 or 24 Niskin bottles to sample seawater for biogeochemical measurements. Water column
98 concentrations of ammonium (NH₄⁺), during both cruises were measured on board as well as nitrate + nitrite (NO₃⁻ +
99 NO₂⁻) concentrations during the GEOVIDE expedition. During the BG2014/14 cruise, samples dedicated for NO₃⁻ +
100 NO₂⁻ and phosphate (PO₄³⁻) measurements were filtered (0.2 μm) and stored at -20°C until analyses at the home-based
101 laboratory. PO₄³⁻ data are not yet available for the GEOVIDE cruise.

102 Nutrient concentrations were determined using conventional fluorometric (for NH₄⁺) (Holmes et al., 1999) and
103 colorimetric methods (for all others) (Grasshoff et al., 1983) with detection limits (DL) of 64 nmol L⁻¹ (NH₄⁺), 90 nmol L⁻¹
104 (NO₃⁻ + NO₂⁻) and 60 nmol L⁻¹ (PO₄³⁻). For the BG2014/14 cruise, chlorophyll *a* (Chl *a*) concentrations were
105 determined according to Yentsch and Menzel (1963), by filtering 250 mL of seawater sample onto Whatman GF/F glass
106 fiber filters (0.7 μm nominal pore size), followed by pigment extraction in 90% acetone, centrifugation and fluorescence
107 measurement using a Shimadzu RF-150 fluorometer. For the GEOVIDE cruise, chlorophyll and carotenoid pigments
108 were determined as described in Ras et al. (2008): 2.3 L of seawater samples were filtered onto Whatman GF/F glass
109 fiber filters, followed by extraction in 100% methanol, disrupted by sonication, clarified by filtration (Whatman GF/F)
110 and analyzed by High-performance liquid chromatography (HPLC, Agilent Technologies system).

111



112 2.2 $^{15}\text{N}_2$ fixation and $^{13}\text{C}\text{-HCO}_3^-$ uptake rates

113 N_2 fixation and primary production (PP) were determined simultaneously in duplicate using the $^{15}\text{N}\text{-N}_2$ dissolution
114 method (Großkopf et al., 2012) and $^{13}\text{C}\text{-NaHCO}_3$ tracer addition (Hama et al., 1983) techniques. Seawater samples were
115 collected in 4.5 L acid-cleaned polycarbonate (PC) bottles from a minimum of four depths (six at stations Geo-1, Geo-13
116 and Geo-21) equivalent to 54%, 13%, 3% and 0.2% of surface PAR (plus 25% and 1% PAR for the 3 exceptions). Details
117 concerning the applied $^{15}\text{N}_2$ dissolution method can be found in Fonseca-Batista et al. (2017). Briefly, $^{15}\text{N}_2$ -enriched
118 seawater was prepared by degassing prefiltered (0.2 μm) seawater, thereafter stored in 2 L gastight Tedlar bags (Sigma-
119 Aldrich) subsequently injected with 30 mL of pure $^{15}\text{N}_2$ gas (98 ^{15}N atom%, Eurisotop, lot number 23/051301) and left to
120 equilibrate. This $^{15}\text{N}_2$ gas batch (Eurisotop) has previously been shown to be free of ^{15}N -labelled contaminants such as
121 nitrate, nitrite, ammonium and nitrous oxide. Each incubation PC bottle was partially filled with sampled seawater, then
122 amended with 250 mL of $^{15}\text{N}_2$ -enriched seawater, spiked with 3 mL of a $\text{NaH}^{13}\text{CO}_3$ solution (200 mmol L^{-1} , 99%,
123 Eurisotop) and topped off with the original seawater sample. Samples were incubated for 24 hours in on-deck incubators
124 circulated with surface seawater and wrapped with neutral density screens (Rosco) simulating the in situ irradiance
125 conditions. After incubation, samples were filtered onto pre-combusted MGF filters (glass microfiber filters, 0.7 μm ,
126 Sartorius), which were subsequently dried at 60°C and stored at room temperature. The natural concentration and isotopic
127 composition of particulate organic carbon and particulate nitrogen (POC and PN) were assessed by filtering an additional
128 4.5 L of non-spiked seawater from each depth. All samples were measured for POC and PN concentrations and isotopic
129 compositions using an elemental analyzer (EuroVector Euro EA 3000) coupled to an isotope mass spectrometer (Delta V
130 Plus, Thermo Scientific) and calibrated against international certified reference material (CRM): IAEA-N1 and IAEA-
131 305B for N and IAEA-CH6 and IAEA-309B for C. N_2 fixation and carbon uptake volumetric rates were computed as
132 described in Montoya et al. (1996), and depth-integrated rates were calculated by non-uniform gridding trapezoidal
133 integration for each station. Minimal detectable uptake rates were determined as detailed in Fonseca-Batista et al. (2017).
134 To do so, the minimal acceptable ^{15}N or ^{13}C enrichment of PN or POC after incubation (Montoya et al., 1996) is
135 considered to be equal to the natural isotopic composition, specific to each sampled depth, increased by three times the
136 uncertainty obtained for N and C isotopic analysis of CRM. All remaining experiment-specific terms are then used to
137 recalculate the minimum detectable uptake. Carbon uptake rates were always above their specific DL, while N_2 fixation
138 was undetectable for some incubations, see details in section 3.3.

139

140 2.3 DNA sampling and *nifH* diversity analysis

141 During the BG2014/14 cruise, water samples used for $^{15}\text{N}_2$ and $\text{NaH}^{13}\text{CO}_3$ incubations were also collected for DNA
142 extraction prior to incubation. 2 L volumes were vacuum filtered (20 to 30 kPa) through 0.2 μm sterile cellulose acetate
143 filters (47 mm Sartorius type 111) subsequently placed in cryovials directly flash deep frozen in liquid nitrogen. At the
144 land-based laboratory, samples were transferred to a -80°C freezer until nucleic acid extraction. DNA was extracted from
145 the samples using the Power Water DNA Isolation kit (MOBIO) and checked for integrity by agarose gel electrophoresis.
146 The amplification of *nifH* sequences was performed on 3–50 $\text{ng } \mu\text{L}^{-1}$ environmental DNA samples using one unit of Taq
147 polymerase (5PRIME), by nested PCR according to Zani et al. (2000) and Langlois et al. (2005).
148 Amplicons of the predicted 359-bp size observed by gel electrophoresis were cloned using the PGEM T Easy cloning kit
149 (PROMEGA) according to the manufacturer's instructions. A total of 103 clones were sequenced by the Sanger technique



150 (GATC, Marseille). DNA alignments were performed using the Molecular Evolutionary Genetics Analysis software
151 (MEGA 7.0) (Kumar et al., 2016) and *nifH* operational taxonomic units (*nifH*-OTUs) were defined with a 5% divergence
152 cutoff. DNA sequences were translated into amino acid sequences, then *nifH* evolutionary distances which are considered
153 as the number of amino acid substitutions per site, were computed using the Poisson correction method (Nei, 1987). All
154 positions containing gaps and missing data were eliminated (see phylogenetic tree in Supporting Information Figure S1).
155 One sequence of each *nifH*-OTU was deposited in GenBank under the accession numbers referenced from KY579322 to
156 KY579337.
157

158 3 Results

159 3.1 Ambient environmental settings

160 Sites sampled in May 2014 during the Belgica BG2014/14 and GEOVIDE cruises, were located within the Iberian Basin
161 Portugal Current System (PCS) (Ambar and Fiúza, 1994) which is influenced by highly fluctuating wind stress (Frouin et
162 al., 1990).

163 The predominant upper layer water mass in this basin is the Eastern North Atlantic Central Water (ENACW), a winter
164 mode water which consists of two components according to Fiúza (1984) (see θ/S diagrams, Figure 2): (i) the lighter,
165 relatively warm and salty ENACWst formed in the subtropical Azores Front region ($\sim 35^\circ$ N) when Azores Mode Water is
166 subducted as a result of strong evaporation and winter cooling; and (ii) the colder and less saline ENACWsp, underlying
167 the ENACWst, and formed in the subpolar eastern North Atlantic (north of 43° N) through winter cooling and deep
168 convection (McCartney and Talley, 1982). The spatial distribution of these Central Waters allowed categorizing the
169 sampling sites in 2 groups: (i) ENACWsp stations north of 43° N (Bel-3, Bel-5, Bel-7, and Geo-21) only affected by the
170 ENACWsp (Figures 2a and 2b) and (ii) ENACWst stations, south of 43° N, characterized by the upper layer being
171 influenced by ENACWst and the subsurface layer by ENACWsp (Figures 2a and 2b). Some of these ENACWst stations
172 are open ocean sites (Bel-9, Bel-11, Bel-13, and Geo-13) while others are shelf-influenced (Geo-1 and Geo-2) (Tonnard
173 et al., 2018).

174 Surface waters of all the ENACWst stations showed a relatively strong stratification resulting from the progressive spring
175 heating, with sea surface temperature (SST) ranging from 15.3 (Geo-13) to 17.2°C (Bel-13). Nutrients were depleted at
176 the surface ($\text{NO}_3^- + \text{NO}_2^- < 0.09 \mu\text{M}$ in the upper 20 m; Figures 3c and 3f) and surface Chl *a* concentrations were low ($<$
177 $0.25 \mu\text{g L}^{-1}$; Figures 3a and 3d) but showed a subsurface maximum (between 0.5 and $0.75 \mu\text{g L}^{-1}$ at approximately 50 m),
178 a common feature for oligotrophic open ocean waters. Amongst the ENACWst stations, station Geo-13 had a slightly
179 higher nutrient content ($\text{NO}_3^- + \text{NO}_2^- = 0.7 \mu\text{M}$ in the lower mixed layer depth, MLD) and higher Chl *a* ($> 0.5 \mu\text{g L}^{-1}$ in
180 the upper 35 m).

181 Surface waters at ENACWsp stations were less stratified (SST between 14.0 and 14.5°C), were nutrient replete (surface
182 $\text{NO}_3^- + \text{NO}_2^-$ ranging from 0.3 to $0.8 \mu\text{M}$) and had a higher phytoplankton biomass (Chl *a* between 0.7 to $1.2 \mu\text{g L}^{-1}$ in the
183 upper 30 m except for station Bel-5). Highest Chl *a* values were observed at station Bel-7 (44.6° N, 9.3° W), which
184 appeared to be located within an anticyclonic mesoscale eddy, as evidenced by the downwelling structure detected in the
185 Chl *a* and $\text{NO}_3^- + \text{NO}_2^-$ profiles (Figures 3a and 3c) at this location (as well as T and S sections, data not shown).

186



187 3.2 Primary production and pigment distribution

188 Volumetric rates of carbon uptake ranged from 7 to 3500 $\mu\text{mol C m}^{-3} \text{d}^{-1}$ (see Supporting Information Table S1) and
189 euphotic layer integrated rates from 32 to 137 $\text{mmol C m}^{-2} \text{d}^{-1}$ (Figure 4 and Supporting Information Table S2).
190 PP was relatively homogenous in the Bay of Biscay (stations Bel-3, Bel-5 and Bel-7) and along the Iberian Margin (Bel-
191 9, Bel-11, Bel-13 and Geo-1) with average rates ranging from 33 to 43 $\text{mmol C m}^{-2} \text{d}^{-1}$, except at station Bel-7 where it
192 was slightly higher (52 $\text{mmol C m}^{-2} \text{d}^{-1}$; Figure 4 and Supporting Information Table S2), likely due to the presence of an
193 anticyclonic mesoscale structure at this location. PP increased westwards away from the Iberian Peninsula, reaching
194 highest values at stations Geo-13 and Geo-21 (79 to 135 $\text{mmol C m}^{-2} \text{d}^{-1}$, respectively; Figure 4) as well as closer to the
195 shelf (reaching 59 $\text{mmol C m}^{-2} \text{d}^{-1}$ at Geo-2). These results are in the range of past measurements for the same period of
196 the year, ranging from 19 to 103 $\text{mmol C m}^{-2} \text{d}^{-1}$ (Marañón et al., 2000; Fernández et al., 2005; Poulton et al., 2006). Our
197 observations also coincide with the area-averaged Chl *a* time series obtained from satellite data (from the Giovanni online
198 data system; Figure 5) which reveal that post bloom conditions prevailed at most sites (Bel-3 to Bel-13 and Geo-1 to Geo-
199 13) while the bloom was still ongoing at station Geo-21 at the time of our study. Higher PP rates appear to coincide with
200 the increase, offshore and towards the shelf, of the relative abundance of diatoms, based on fucoxanthin pigment
201 concentrations (Figure 6) (Tonnard et al., in preparation for this Special issue). At the less nutrient replete GEOVIDE
202 sites Geo-1 and Geo-13, prymnesiophytes represented 30–40% of the phytoplankton community, compared to 20–35% at
203 stations Geo-21 and Geo-2 (based on the presence of 19'-hexanoyloxyfucoxanthin pigment). Such relative abundances
204 are in agreement with the global abundance of prymnesiophytes ($32 \pm 5\%$) proposed by Swan et al. (2016).
205

206 3.3 Diazotrophic activity and diversity

207 Where detectable, volumetric N_2 fixation rates ranged from 0.7 to 65.4 $\text{nmol N L}^{-1} \text{d}^{-1}$ (see Supporting Information Table
208 S1), with areal rates ranging between 81 and 1533 $\mu\text{mol N m}^{-2} \text{d}^{-1}$ (Figure 7 and Supporting Information Table S2).
209 We observed very high N_2 fixation activities at the two sites (Bel-11 and Bel-13) most affected by ENACW waters of
210 subtropical origin (Figure 2). There, volumetric rates of N_2 fixation ranged from 2.4 to 65.4 $\text{nmol N L}^{-1} \text{d}^{-1}$ and average
211 areal rates from 1355 to 1533 $\mu\text{mol N m}^{-2} \text{d}^{-1}$. We were able to recover from the BG2014/14 cruise 103 *nifH* sequences
212 (from positive PCR amplifications) in surface waters (54% PAR level) of stations Bel-11 and Bel-13. No successful *nifH*
213 amplifications were obtained at other stations and depths where diazotrophic activities were lower. At station Bel-11, a
214 single OTU was recovered as all *nifH* sequenced clones ($n = 41$) had 99% similarity at the nucleotide level and 100%
215 similarity at the amino acid level with *Candidatus Atelocyanobacterium thalassa* isolate (heterotrophic diazotrophic
216 cyanobacteria, UCYN-A1; Figures 8A and S1) from station ALOHA in the North Pacific (Thompson et al., 2012).
217 Station Bel-13 illustrated an apparent greater diversity, as indicated by the 15 OTUs recovered there (from 62 sequenced
218 clones; Figures 8A–B and S1) and their percentage contribution to the Chao 1 estimates of total *nifH*-OTUs reaching 17.5
219 for this station. The latter species richness index gives an estimate of total number of species for a given community,
220 based on the number of singleton (OTU represented by a single read) and doubletons (OTU obtained twice) found in the
221 sample (Chao, 1984). This suggests that for Bel-13, recovered OTUs could explain 85.7% of the diversity. Among these
222 15 OTUs, 45.2% of the sequences were affiliated to UCYN-A1 (identical to those found at Bel-11), and the rest to
223 heterotrophic bacteria with 25.8% affiliated to Bacteroidetes, 19.3% to Firmicutes and 9.7% to Proteobacteria (Figures
224 8A and S1).



225 Shelf-influenced (Geo-1 and Geo-2) and open ocean (Geo-13) ENACWst sites, besides Bel-11 and Bel-13, displayed
226 relatively high N_2 fixation activities with volumetric rates ranging between 1.0 and 7.1 $\text{nmol N L}^{-1} \text{d}^{-1}$ (Supporting
227 Information Table S1) and average depth-integrated rates of 141, 262 and 384 $\mu\text{mol N m}^{-2} \text{d}^{-1}$, respectively (Figure 7 and
228 Supporting Information Table S2). N_2 fixation was also high at the most productive ENACWsp sites Bel-7 and Geo-21
229 with volumetric rates ranging from 1.0 to 8.2 $\text{nmol N L}^{-1} \text{d}^{-1}$ and average areal rates of 128 and 279 $\mu\text{mol N m}^{-2} \text{d}^{-1}$,
230 respectively. However, no diazotrophic activity was measured at ENACWsp sites Bel-3 and Bel-5 in the central Bay of
231 Biscay nor at specific depths of stations Bel-9 (120 m), Bel-11 (45 m) and Geo-21 (18 m).

232 We computed the relative contribution of N_2 fixation to PP by converting N_2 fixation rates to carbon uptake using either a
233 Redfield ratio of 6.6 or the determined median POC/PN ratio for natural particles (equivalent to the mean value of $6.3 \pm$
234 1.1 , \pm SD, $n = 46$; Table 1). N_2 fixation contributed to less than 2% of PP in the ENACWsp sites and between 3 to 28% of
235 PP in the southernmost ENACWst sites, except at station Bel-9 where it supported about 1% of PP. These contributions
236 reach values twice as high as those reported in other studies for the oligotrophic tropical and subtropical eastern Atlantic
237 usually considered as systems prone to host diazotrophic activity (contributions to PP ranging from $< 1\%$ to 12%) (Voss
238 et al., 2004; Rijkenberg et al., 2011; Fonseca-Batista et al., 2017). However, it is important to keep in mind that this
239 computation relies on the assumption that only photoautotrophic diazotrophs contribute to bulk N_2 fixation, which is not
240 always the case, particularly in the present study.

241

242 4 Discussion

243 During two expeditions to the Iberian Basin and Bay of Biscay in May 2014 (38.8–46.5° N), we observed N_2 fixation
244 activity in surface waters of most stations (except at the two northernmost sites in the Bay of Biscay), characterized by
245 relatively low SST (12.5–17.3°C) and a wide range of DIN concentrations ($\text{NO}_3^- + \text{NO}_2^-$ from < 0.1 to 7.6 μM). In the
246 following sections we discuss (1) the major contributors to diazotrophic activity in these high latitude regions, (2) the
247 significance of N_2 fixation in the Iberian Basin, and to a wider extent in the whole Atlantic, and (3) the potential
248 environmental drivers of the unexpectedly high diazotrophic activity in the Iberian Basin.

249

250 4.1 Features of the diazotrophic community composition in the temperate North Atlantic

251 Diazotrophic diversity investigation during the Belgica BG2014/14 cruise (stations Bel-3 to Bel-13) revealed the presence
252 of *nifH* sequences only in the surface waters of ENACWst stations Bel-11 and Bel-13, where we observed the highest
253 areal N_2 fixation rates, exceeding 1000 $\mu\text{mol N m}^{-2} \text{d}^{-1}$ (Figures 7 and 8). Our qualitative assessment of *nifH* diversity
254 suggested a predominant role of heterotrophic diazotrophs (UCYN-A as the singular cyanobacterial phylotype and non-
255 cyanobacterial diazotrophs) and the lack of presence of *Trichodesmium* filaments. These findings are corroborated by the
256 more quantitative assessment of *nifH* diversity carried out at stations Geo-1, Geo-2, Geo-13 and Geo-21 (Julie LaRoche,
257 personal communication, 2018) confirming that only heterotrophic non-cyanobacterial phylotypes contributed to the
258 observed N_2 fixation activity. For the BG2014/14 cruise, UCYN-A1 represented 67% of all *nifH* sequences recovered off
259 the Iberian Margin, with the remainder sequences belonging to non-cyanobacterial groups (Bacteroidetes, Firmicutes and
260 Proteobacteria). Previous work in temperate regions of the global ocean (Needoba et al., 2007; Rees et al., 2009;



261 Mulholland et al., 2012; Shiozaki et al., 2015) including the Iberian Margin (Agawin et al., 2014; Moreira-Coello et al.,
262 2017) also reported that highest N₂ fixation activities were predominantly related to the presence of UCYN-A cells
263 (UCYN-A1, UCYN-A2 and UCYN-A3 clades being only identified a posteriori) (Thompson et al., 2014) and
264 heterotrophic bacteria, while *Trichodesmium* filaments were low or undetectable.

265 UCYN-A cells (in particular from the UCYN-A1 clade) were shown to live in mutualistic symbioses with single-celled
266 prymnesiophyte algae (Thompson et al., 2012). This symbiotic association was believed to be obligate since UCYN-A
267 are characterized by an unusually streamlined genome lacking essential cyanobacterial features such as the photosystem
268 II, the RuBisCo and the tricarboxylic acid cycle (Zehr et al., 2008; Tripp et al., 2010). The prymnesiophyte-UCYN-A1
269 symbiosis was consistently observed during the work of Cabello et al. (2015) across the global ocean and is thus being
270 considered as an obligate association. In addition, this symbiosis has been reported to be particularly abundant in the
271 central and eastern basin of the North Atlantic (Krupke et al., 2014; Cabello et al., 2015), which is consistent with the fact
272 that a relatively important proportion of prymnesiophyte species were observed in that region during the GEOVIDE
273 cruise (Figure 6).

274 Bacteroidetes, commonly encountered in the marine environment, are considered as specialized degraders of organic
275 matter that preferably grow attached to particles or algal cells (Fernández-Gómez et al., 2013). Studies have shown the
276 presence of N₂ fixation and/or nitrogenase-like genes (among which *nifH* and/or *nifD*) in the genome of several species of
277 this phylum (Dos Santos et al., 2012; Inoue et al., 2015). Furthermore, N₂ fixation activity has been reported in five
278 Bacteroidetes strains including *Bacteroides graminisolvens*, *Paludibacter propionigenes* and *Dysgonomonas gadei*
279 (Inoue et al., 2015) which are the closest cultured relatives of the *nifH*-OTUs detected at station Bel-13 (Figure S1). The
280 remaining sequences were affiliated to Cluster III phylotypes of functional nitrogenase genes, which mainly consist of
281 anaerobic bacteria containing molybdenum nitrogenase genes such as *Clostridium* (Firmicutes), *Desulfovibrio*
282 (Deltaproteobacteria), *Sulfurospirillum* (Epsilonproteobacteria) (Chien and Zinder, 1996). Anaerobic Cluster III
283 phylotypes have been previously recovered from different ocean basins (Church et al., 2005; Langlois et al., 2005, 2008;
284 Man-Aharonovich et al., 2007; Rees et al., 2009; Halm et al., 2012; Mulholland et al., 2012). These diazotrophs were
285 suggested to benefit from anoxic microzones found within marine snow particles or zooplankton guts to fix N₂ thereby
286 avoiding oxygenic inhibition of their nitrogenase enzyme (Braun et al., 1999; Church et al., 2005; Scavotto et al., 2015).
287 Therefore, the bloom to early post bloom conditions prevailing during our study, probably constituted an ideal condition
288 for diazotrophic groups that depend on the availability of detrital organic matter availability or association with grazing
289 zooplankton.

290 No *Trichodesmium* filaments were recovered during the BG2014/14 cruise, nor during GEOVIDE sampling in the Iberian
291 region, although *Trichodesmium* spp. have recently been reported to be widely distributed in temperate waters of the
292 North Atlantic (Rivero-Calle et al., 2016). Despite the fact that our sampling strategy (Niskin sampling) is not suited for a
293 quantitative recovery of *Trichodesmium* (Montoya et al., 2007), it is likely that any presence of filaments would still have
294 been detected had they been present at the time of our field investigation. This was also confirmed by a CHEMTAX
295 analysis of pigments (Tonnard et al., in preparation for this Special issue).

296 Our findings further support the important role played by small diazotrophs, particularly heterotrophic groups, in
297 introducing new N to the oceanic budget. These observations tend to comfort the idea of a substantial role played not only
298 by UCYN-A (Cabello et al., 2015; Martínez-Pérez et al., 2016) but also by non-cyanobacteria (Halm et al., 2012;



299 Shiozaki et al., 2014; Langlois et al., 2015) in oceanic N₂ fixation. However, while these authors mostly reported on the
300 widespread distribution of these specific groups of diazotrophs, their in situ activity yet remains poorly quantified.

301

302 **4.2 Significance of N₂ fixation in the temperate ocean**

303 In the present study, we found surprisingly high N₂ fixation activities at most of the studied sites. Rates were
304 exceptionally elevated at two open ocean sites located between 38.8–40.7° N at about 11° W (averaging 1533 and 1355
305 $\mu\text{mol N m}^{-2} \text{d}^{-1}$ at stations Bel-11 and Bel-13, respectively; Figure 7 and Tables S1 and S2). Although N₂ fixation was not
306 detected in the central Bay of Biscay (stations Bel-3 and Bel-5), rates recorded at all the other sites were relatively high,
307 not only in shelf-influenced areas (141 and 262 $\mu\text{mol N m}^{-2} \text{d}^{-1}$ at stations Geo-1 and Geo-2, respectively) but also in the
308 open ocean (average activities between 81–384 $\mu\text{mol N m}^{-2} \text{d}^{-1}$ at stations Bel-7, Bel-9, Geo-13 and Geo-21).

309 Previous studies in the Iberian Basin (35–50° N, east of 25° W) reported relatively lower N₂ fixation rates (from < 0.1 to
310 140 $\mu\text{mol N m}^{-2} \text{d}^{-1}$), regardless of whether the bubble-addition method of Montoya et al. (1996) or the dissolution
311 method by Mohr et al. (2010) and Großkopf et al. (2012) were used. However, these studies were carried out largely
312 outside the bloom period, either during the late growth season (summer and autumn) (Moore et al., 2009; Benavides et
313 al., 2011; Snow et al., 2015; Riou et al., 2016; Fonseca-Batista et al., 2017) or during winter (Rijkenberg et al., 2011;
314 Agawin et al., 2014). In contrast, the present study took place in spring, during or just at the end of the vernal
315 phytoplankton bloom. Differences in timing of these different studies and to a lesser extent, differences in applied
316 methodologies (bubble-addition relative to the dissolution method) may explain the discrepancies in diazotrophic activity
317 observed between our study and earlier works.

318 Our values are either similar or up to one order of magnitude higher than maximal N₂ fixation rates reported for the
319 eastern tropical and subtropical North Atlantic further south (reaching up to 360–424 $\mu\text{mol N m}^{-2} \text{d}^{-1}$) (Großkopf et al.,
320 2012; Subramaniam et al., 2013; Fonseca-Batista et al., 2017). Yet, conditions favouring N₂ fixation are commonly
321 believed to be met in these tropical and subtropical regions of the North Atlantic: (1) intense Saharan dust deposition
322 providing dissolved iron (dFe), a co-factor of the nitrogenase enzyme (Raven, 1988; Howard and Rees, 1996); (2)
323 stronger stratification (resulting in DIN-depleted surface waters) (Capone et al., 2005; Luo et al., 2014) and (3) input via
324 eastern boundary upwelling of subsurface waters carrying excess of PO₄³⁻ relative to NO₃⁻ (i.e., excess relative to the
325 canonical Redfield P/N ratio; expressed as P*). This positive P* signature in subsurface waters of the Atlantic Ocean is
326 considered to originate either from the Indo-Pacific (Deutsch et al., 2007; Moore et al., 2009; Ratten et al., 2015;
327 Fonseca-Batista et al., 2017) or the Arctic (Yamamoto-Kawai et al., 2006).

328 In the Atlantic Ocean, very high N₂ fixation rates up to ~1000 $\mu\text{mol N m}^{-2} \text{d}^{-1}$ as observed here, have only been reported
329 for temperate coastal waters of the Northwest Atlantic (up to 838 $\mu\text{mol N m}^{-2} \text{d}^{-1}$) (Mulholland et al., 2012) and for
330 tropical shelf-influenced and mesohaline waters of the Caribbean and Amazon River plume (maximal rates ranging
331 between 898 and 1600 $\mu\text{mol N m}^{-2} \text{d}^{-1}$) (Capone et al., 2005; Montoya et al., 2007; Subramaniam et al., 2008). Shelf and
332 mesohaline areas have indeed been shown to harbor considerable N₂ fixation activity, not only in tropical regions
333 (Montoya et al., 2007; Subramaniam et al. 2008) but also in areas from temperate to polar regions (Rees et al., 2009;
334 Blais et al., 2012; Mulholland et al., 2012; Shiozaki et al., 2015). Yet, the environmental features which enhance
335 diazotrophic activity in those regions are not fully understood. For tropical mesohaline systems the conditions proposed to
336 drive such an intense diazotrophic activity include the occurrence of highly competitive symbiosis, i.e. diatom-



337 diazotrophs associations, besides the influence of a positive P^* input from the Amazon River (Subramaniam et al., 2008).
338 However, such conditions of excess P were however not observed in the present study (see section 4.3) nor in previous
339 studies carried out in high latitude shelf regions with elevated N_2 fixation activities (Blais et al., 2012; Mulholland et al.,
340 2012; Shiozaki et al., 2015). In addition, while tropical mesohaline regions are characterized by the predominance of
341 diatom-diazotroph associations (and filamentous *Trichodesmium* spp.), in temperate shelf areas the diazotrophic
342 community is reported to be essentially dominated by heterotrophic diazotrophs, from UCYN-A symbionts of
343 prymnesiophyte algae to Proteobacteria and Cluster III phylotypes (Rees et al., 2009; Blais et al., 2012; Mulholland et al.,
344 2012; Agawin et al., 2014; Shiozaki et al., 2015).
345 We propose that bloom-related processes are partly responsible for the unprecedented high N_2 fixation rates observed in
346 the Iberian region at the time of our study. In the next section, we investigate environmental drivers which could, in
347 combination with the latter, explain the large range of N_2 fixation rates observed in the present study (from undetectable
348 rates up to $1533 \mu\text{mol N m}^{-2} \text{d}^{-1}$).
349

350 4.3 Key environmental drivers of N_2 fixation

351 In the past decades, the study of environmental factors regulating marine N_2 fixation has specifically focused on
352 autotrophic cyanobacteria as these were generally believed to be the most active diazotrophs (Zehr et al., 2001; Luo et al.,
353 2014). Nevertheless, the commonly recognized environmental controls such as solar radiation, sea surface temperature,
354 DIN and dissolved oxygen concentration (Luo et al., 2014), may not directly affect the heterotrophic diazotrophs. Indeed
355 by having fundamentally different ecologies relative to autotrophic diazotrophs, heterotrophic diazotrophs are expected to
356 exhibit discrete regulation of their N_2 fixation activity (Bombar et al., 2016). Nonetheless, molecular and cellular
357 conditions for sustaining N_2 fixation activity and related processes still requires the supply of dFe and P (Raven, 1988;
358 Howard and Rees, 1996). DFe and P availability (Mills et al., 2004; Moore et al., 2009) as well as positive P^* signature
359 (Deutsch et al., 2007; Moore et al., 2009; Ratten et al., 2015; Fonseca-Batista et al., 2017) are in fact considered to
360 regulate the distribution of bulk oceanic N_2 fixation. Besides these critical inorganic nutrients, heterotrophic N_2 fixation
361 was also recently shown to be highly dependent on the availability of organic matter (Bonnet et al., 2013; Rahav et al.,
362 2013, 2016; Loescher et al., 2014).

363 In the present study we hypothesize that seasonality of phytoplankton production is a major driver of N_2 fixation in the
364 Iberian Margin. Since surface waters at the time of our study were under bloom to post-bloom conditions, they likely
365 carried significant amounts of organic matter which may have promoted the growth of heterotrophic diazotrophs. This
366 hypothesis is supported by findings from the GEOVIDE cruise showing that surface waters of the Iberian Basin (stations
367 Geo-1 and Geo-13) and the West European Basin (Geo-21) illustrated rather variable but significant upper column (100–
368 120 m) particulate organic carbon concentration (POC of 166, 171 and $411 \text{ mmol C m}^{-2}$, respectively) with a dominant
369 fraction of small size POC (1–53 μm) relative to total abundance (75%, 92% and 64%, respectively) (Lemaitre et al.,
370 2018). Small cells, usually being slow-sinking particles, are considered easily remineralized in surface waters (Villa-
371 Alfageme et al., 2016) which was confirmed by the very low export efficiency observed at stations Geo-13 and Geo-21
372 (3% and 4% of euphotic layer integrated PP reaching the depth of export, respectively) evidencing an efficient shallow
373 remineralisation (due to bacterial and zooplankton activity). Although the upper 100 m at station Geo-1 was characterized
374 by a less effective recycling of organic matter (export efficiency of 35%), likely due to lithogenic ballast effect and to the



375 presence of larger and/or denser phytoplankton groups, export efficiency there may have been overestimated to an
376 unusually low in situ PP (relative to satellite-based estimates) (Lemaitre et al., 2018). Therefore, we pose secondly that
377 the availability of organic matter in the upper layers likely contributed to supplying remineralized P (organic P being
378 generally more labile than other organic nutrients) (Vidal et al., 1999, 2003) and to enhancing the residence time of dFe
379 originated from atmospheric deposition. These conditions all together would benefit the heterotrophic N₂ fixers.
380 Despite the fact that neither P* values from the BG2014/14 cruise (Table S1) nor climatological P* data for the Iberian
381 Basin (World Ocean Atlas 2013 April to June average from 1955 to 2012, Figure 1 and Table S2) (Garcia et al., 2013)
382 indicate a large PO₄³⁻ excess (P* ranging between -0.1 and 0.1 μmol L⁻¹; Figure 1 and Tables S1 and S2). Spearman rank
383 correlations suggest that volumetric N₂ fixation rates were significantly correlated with the BG2014/14 shipboard P*
384 values ($p < 0.01$). However, ENACWst stations Bel-11 and Bel-13 are weighing heavily in this correlation, and without
385 the data from these two sites the correlation is no longer significant ($p = 0.163$). Landolfi et al. (2015) proposed that in
386 waters depleted in DIN and PO₄³⁻ and devoid of a positive P* signal, but replete in dFe, the ability of diazotrophs to draw
387 N from the dissolved N₂ pool confers them a competitive advantage over other phytoplankton for the use of dissolved
388 organic phosphorus (DOP). According to Landolfi et al., the need for additional N and energy required for the enzymatic
389 mineralization of DOP (synthesis of extracellular alkaline phosphatase) favors N₂ fixers in such oligotrophic conditions,
390 and such DOP utilization by diazotrophs has been reported in other studies for the North Atlantic (Dyhrman et al., 2006;
391 Sohm and Capone, 2006; Moore et al., 2009). In case DOP had progressively accumulated towards the end of the spring
392 bloom, it may have contributed to sustaining N₂ fixation in the studied region.
393 Atmospheric aerosol deposition determined during the GEOVIDE cruise (Shelley et al., 2017) as well as the satellite-
394 based dust deposition values averaged over the month of May (Figure S3; Giovanni online satellite data system, NASA
395 Goddard Earth Sciences Data and Information Services Center), both reveal weak dust loadings over the Iberian region at
396 the time of sampling. While euphotic layer-integrated N₂ fixation rates determined during both GEOVIDE and
397 BG2014/14 cruises were negatively correlated with average May dust input ($p < 0.01$, Table S3), they tended to be
398 positively correlated with the average dust input during the month preceding the field work (April). This correlation,
399 though weak ($p = 0.45$, Table S3), suggests an availability of dFe in May likely resulting from the intense atmospheric
400 dust input in the preceding month which affected the area studied here as well as the area more to the south. Indeed, it has
401 been reported that dFe in surface waters (50 to 100 m deep) of the North Atlantic may remain available to the microbiota
402 up to a month after the atmospheric dust deposition events, most likely due to the formation of ligands with dissolved
403 organic components (Jickells, 1999; de Baar and de Jong, 2001; Sarthou et al., 2003). In addition it is likely that dFe was
404 also supplied at the time of our sampling through lateral advection from the continental margin (for stations Geo-1 and
405 Geo-2) as indicated by the surface salinity minima (Figures 2b and 2c) and the low dFe to dissolved aluminium ratios
406 found there relative to surrounding waters (Tonnard et al., 2018). Also, dFe could have been supplied from the adjacent
407 subtropical region more heavily impacted by the April dust deposition (stations Bel-11, Bel-13 and Geo-13). In addition,
408 it is important to note that vertical mixing (related to post-winter convection) with Fe-enriched subsurface waters
409 (Thuróczy et al., 2010; Rijkenberg et al., 2012; García-Ibáñez et al., 2015) could also have supplied dFe particularly at
410 station Geo-21 (to a lesser extent at Geo-13) where the surface waters showed rather nutrient replete conditions (Figure
411 3).
412 θ/S diagrams at stations Bel-11 and Bel-13 (and to a lesser extent at Geo-13) reveal the presence of very warm and saline
413 waters at the surface and which appear to be advected from subtropical regions in the south, as indicated by SST satellite



414 images (Figure S2). Spearman rank correlations (Table S4) confirm that N_2 fixation rates increased towards elevated
415 seawater temperature ($p < 0.001$) and $NO_3^- + NO_2^-$ depleted surface waters ($p < 0.05$). We thus propose that N_2 fixation
416 activity at stations Bel-11 and Bel-13, where rates were the highest, was stimulated by the northward advection of
417 subtropical surface waters which would have received a larger supply of dFe from dust deposition (Figure S3A) and
418 which carried positive P^* signatures. Alternatively, these northward flowing waters could have conveyed active
419 diazotrophs of subtropical origin. Shiozaki et al. (2013) reported a similar feature for the western North Pacific, where
420 diazotrophic cyanobacteria were carried along warm surface currents while conserving their N_2 fixation potential. In
421 contrast, in the central Bay of Biscay N_2 fixation was below detection limit at stations Bel-3 and Bel-5 (45.3–46.5° N)
422 while it was still significant further offshore at similar latitude (station Geo-21, 46.5° N; Figure 7). During April 2014,
423 dust deposition was lowest in the region of the Bay of Biscay (Figure S3), suggesting that N_2 fixation there might have
424 been limited by dFe availability. This was corroborated by the observation that surface waters from stations Bel-3 and
425 Bel-5, when incubated after dFe amendments, exhibited high N_2 fixation rates ($> 25 \text{ nmol N L}^{-1} \text{ d}^{-1}$; Li et al., 2018).

426 The statements discussed in this section are further supported by the outcome of a multivariate statistical analysis
427 providing a comprehensive view of the environmental features influencing N_2 fixation. A principal component analysis
428 (PCA; Tables 2 and S2) generated two components (or axes) explaining 68% of the system's variability. Axis 1 illustrates
429 the productivity of the system, or more precisely the oligotrophic state towards which it is evolving. In fact, axis 1 is
430 defined by a strong positive relation with surface temperature (reflecting the onset of stratification, particularly for
431 stations Bel-11 and Bel-13; Figure 9) and an inverse relation with PP associated variables (PP, Chl a , NH_4^+ , $NO_3^- + NO_2^-$
432). Sites characterized by a moderate (Bel-3 and Bel-5) to high (Bel-7, Geo-21 and to a lesser extent Geo-13) primary
433 production appear indeed tightly linked to these PP associated variables as illustrated in Figure 9. As reflected by the
434 positive relation with surface salinity and P^* (Figure 9), axis 2 denotes advection of surface waters of subtropical origin,
435 for stations Bel-11, Bel-13 and Geo-13. For stations Geo-1 and Geo-2, the inverse relation with surface salinity (Figure 9)
436 is interpreted to reflect fluvial inputs (Tonnard et al., 2018). Finally, this statistical analysis indicates that N_2 fixation
437 activity was likely influenced by the two PCA components, tentatively identified as productivity (axis 1) and surface
438 water advection (axis 2) from the shelf and the subtropical region.

439 This investigation into possible drivers of heterotrophic N_2 fixation in the Iberian Margin and Bay of Biscay points to the
440 critical roles played by (i) organic matter availability in these open waters, resulting from the prevailing vernal bloom to
441 post-bloom conditions, in combination with (ii) atmospheric dust deposition providing essential dFe. Further studies are
442 required to investigate this possible link between heterotrophic N_2 fixation activity and phytoplankton bloom in the
443 studied region. It is likely that surface water advection also played an important role in supporting N_2 fixation activities
444 by conveying essential nutrients from subtropical regions or shelf areas into the studied region.

445 5 Conclusion

446 The present study highlights the occurrence of high N_2 fixation activity ($81\text{--}1533 \text{ } \mu\text{mol N m}^{-2} \text{ d}^{-1}$) in the temperate
447 eastern North Atlantic off the Iberian Peninsula, under vernal bloom to post bloom conditions. However, no activity was
448 detected in the central Bay of Biscay at the time of this study. We report diazotrophic activities being of similar range to
449 ten times larger compared to those reported by others for the eastern tropical and subtropical North Atlantic. The
450 qualitative assessments of *nifH* diversity in the West Iberian Margin (from BG2014/14 and GEOVIDE cruises) suggest



451 that the diazotrophic community was dominated by heterotrophs, among which the UCYN-A1 obligate symbiont of
452 photo-autotrophic prymnesiophyte cells as well as anaerobic bacteria being particle-associated or zooplankton symbionts,
453 such as Bacteroidetes, Proteobacteria and Firmicutes phylotypes. We postulate that the availability of suspended organic
454 matter (dissolved and/or particulate) related to the ongoing or past phytoplankton bloom promoted heterotrophic N₂
455 fixation activity by sustaining bacterial production, but also by providing sufficient nutrients essential for the nitrogenase
456 activity. Dissolved Fe was supplied mostly through atmospheric dust deposition, and advection from subtropical regions
457 or from the shelf area. The proposed environmental controls support the idea of a closer link between primary production
458 and N₂ fixation in productive areas where accumulation of organic matter would favour the growth of heterotrophic
459 diazotrophs. Further investigations of N₂ fixation activity, organic matter availability and assimilation off the Iberian
460 Margin particularly during productive seasons, are needed to confirm these statements.

461

462 Data availability. The data associated with the paper are available from the corresponding author upon request.

463

464 The Supplement related to this article is available.

465

466 Competing interests. The authors declare that they have no conflict of interest.

467

468

469 *Acknowledgements.* We thank the Captains and the crews of R/V Belgica and R/V “Pourquoi pas?” for their skillful
470 logistic support. A very special thanks goes to the chief scientists G. Sarthou and P. Lherminier of the GEOVIDE
471 expedition for the great work experience and wonderful support on board. We thank A. Roukaerts and D. Verstraeten for
472 their assistance with laboratory tasks at the Vrije Universiteit Brussel. We would like to give a special thanks to Pierre
473 Branellec, Michel Hamon, Catherine Kermabon, Philippe Le Bot, Stéphane Leizour, Olivier Ménage (Laboratoire
474 d’Océanographie Physique et Spatiale), Fabien Péroult and Emmanuel de Saint Léger (Division Technique de l’INSU,
475 Plouzané, France) for their technical expertise during clean CTD deployments. P. Lherminier, P. Tréguer, E. Grossteffan,
476 and M. Le Goff are gratefully acknowledged for providing us with the shipboard physico-chemical data including CTD
477 and nitrate plus nitrite data from the GEOVIDE expedition. Phytoplankton pigment diversity data was supplied by C.
478 Dimier, J. Ras and H. Claustre from the “Service d’Analyse de PIGments par HPLC” (SAPIGH) in the oceanographic
479 laboratory of Villefranche-sur-Mer. We also thank C. Schmechtig for the LEFE-CYBER GEOVIDE database
480 management. Shiptime for the Belgica BG2014/14 cruise was granted by Operational Directorate ‘Natural Environment’
481 (OD Nature) of the Royal Institute of Natural Sciences, Belgium. OD Nature (Ostend) is also acknowledged for their
482 assistance in CTD operations and data acquisition on board the R/V Belgica. This work was financed by Flanders
483 Research Foundation (FWO contract G0715.12N) and Vrije Universiteit Brussel, R&D, Strategic Research Plan “Tracers
484 of Past & Present Global Changes“. Additional funding was provided by the Fund for Scientific Research - FNRS
485 (F.R.S.-FNRS) of the Wallonia-Brussels Federation (convention no. J.0150.15). X. Li was a FNRS doctorate Aspirant
486 fellow. This study was also supported, through the GEOVIDE expedition, by the French National Research Agency
487 (ANR-13-B506-0014), the Institut National des Sciences de L’Univers (INSU) of the Centre National de la Recherche
488 Scientifique (CNRS), and the French Institute for Marine Science (Ifremer). This work was logistically supported for the
489 by DT-INSU and GENAVIR. Finally, this work was also a contribution to the Labex OT-Med [ANR-11-LABEX-0061,



490 www.otmed.fr] funded by the « Investissements d’Avenir », French Government project of the French National Research
491 Agency [ANR, www.agence-nationale-recherche.fr] through the A*Midex project [ANR-11-IDEX-0001-02], funding V.
492 Riou during the preparation of the manuscript.

493 References

- 494 Agawin, N. S. R., Benavides, M., Busquets, A., Ferriol, P., Stal, L. J., & Arístegui, J. (2014). Dominance of unicellular
495 cyanobacteria in the diazotrophic community in the Atlantic Ocean. *Limnology and Oceanography*, 59(2), 623–637.
496 <https://doi.org/10.4319/lo.2014.59.2.0623>
- 497 Benavides, M., Agawin, N., Arístegui, J., Ferriol, P., & Stal, L. (2011). Nitrogen fixation by *Trichodesmium* and small
498 diazotrophs in the subtropical northeast Atlantic. *Aquatic Microbial Ecology*, 65(1), 43–53.
499 <https://doi.org/10.3354/ame01534>
- 500 Benavides, M., & Voss, M. (2015). Five decades of N₂ fixation research in the North Atlantic Ocean. *Frontiers in Marine
501 Science*, 2(June), 1–20. <https://doi.org/10.3389/fmars.2015.00040>
- 502 Blais, M., Tremblay, J.-É., Jungblut, A. D., Gagnon, J., Martin, J., Thaler, M., & Lovejoy, C. (2012). Nitrogen fixation
503 and identification of potential diazotrophs in the Canadian Arctic. *Global Biogeochemical Cycles*, 26(3), 1–13.
504 <https://doi.org/10.1029/2011GB004096>
- 505 Bombar, D., Paerl, R. W., & Riemann, L. (2016). Marine Non-Cyanobacterial Diazotrophs: Moving beyond Molecular
506 Detection. *Trends in Microbiology*, 24(11), 916–927. <https://doi.org/10.1016/j.tim.2016.07.002>
- 507 Bonnet, S., Dekaezemacker, J., Turk-Kubo, K. a, Moutin, T., Hamersley, R. M., Grosso, O., ... Capone, D. G. (2013).
508 Aphotic N₂ fixation in the Eastern Tropical South Pacific Ocean. *PloS One*, 8(12), e81265.
509 <https://doi.org/10.1371/journal.pone.0081265>
- 510 Braun, S. T., Proctor, L. M., Zani, S., Mellon, M. T., & Zehr, J. P. Y. (1999). Molecular evidence for zooplankton-
511 associated nitrogen-fixing anaerobes based on amplification of the *nifH* gene. *FEMS Microbiology Ecology*, 28, 273–
512 279.
- 513 Breitbarth, E., Oschlies, A., & LaRoche, J. (2007). Physiological constraints on the global distribution of *Trichodesmium*
514 – effect of temperature on diazotrophy. *Biogeosciences*, 4, 53–61. <https://doi.org/10.5194/bg-4-53-2007>
- 515 Cabello, A. M., Cornejo-Castillo, F. M., Raho, N., Blasco, D., Vidal, M., Audic, S., ... Massana, R. (2015). Global
516 distribution and vertical patterns of a prymnesiophyte–cyanobacteria obligate symbiosis. *The ISME Journal*, 1–14.
517 <https://doi.org/10.1038/ismej.2015.147>
- 518 Capone, D. G. (1997). *Trichodesmium*, a Globally Significant Marine Cyanobacterium. *Science*, 276(5316), 1221–1229.
519 <https://doi.org/10.1126/science.276.5316.1221>
- 520 Capone, D. G., Burns, J. A., Montoya, J. P., Subramaniam, A., Mahaffey, C., Gunderson, T., ... Carpenter, E. J. (2005).
521 Nitrogen fixation by *Trichodesmium* spp.: An important source of new nitrogen to the tropical and subtropical North
522 Atlantic Ocean. *Global Biogeochemical Cycles*, 19(2), 1–17. <https://doi.org/10.1029/2004GB002331>
- 523 Chao, A. (1984). Nonparametric Estimation of the Number of Classes in a Population. *Scandinavian Journal of Statistics*,
524 11(4), 265–270. <https://doi.org/10.1214/aoms/1177729949>



- 525 Chien, Y.-T., & Zinder, S. H. (1996). Cloning, functional organization, transcript studies, and phylogenetic analysis of
526 the complete nitrogenase structural genes (*nifHDK2*) and associated genes in the archaeon *Methanosarcina barkeri* 227.
527 *Journal of Bacteriology*, 178(1), 143–148.
- 528 Church, M. J., Jenkins, B. D., Karl, D. M., & Zehr, J. P. (2005). Vertical distributions of nitrogen-fixing phylotypes at Stn
529 ALOHA in the oligotrophic North Pacific Ocean. *Aquatic Microbial Ecology*, 38(1), 3–14.
530 <https://doi.org/10.3354/ame038003>
- 531 de Boyer Montégut, C., Madec, G., Fischer, A. S., Lazar, A., & Iudicone, D. (2004). Mixed layer depth over the global
532 ocean: An examination of profile data and a profile-based climatology. *Journal of Geophysical Research C: Oceans*,
533 109(12), 1–20. <https://doi.org/10.1029/2004JC002378>
- 534 Deutsch, C., Sarmiento, J. L., Sigman, D. M., Gruber, N., & Dunne, J. P. (2007). Spatial coupling of nitrogen inputs and
535 losses in the ocean. *Nature*, 445(7124), 163–167. <https://doi.org/10.1038/nature05392>
- 536 Dore, J. E., Brum, J. R., Tupas, L., & Karl, D. M. (2002). Seasonal and interannual variability in sources of nitrogen
537 supporting export in the oligotrophic subtropical North Pacific Ocean. *Limnol. Oceanogr.*, 47(6), 1595–1607.
- 538 Dos Santos, P. C., Fang, Z., Mason, S. W., Setubal, J. C., & Dixon, R. (2012). Distribution of nitrogen fixation and
539 nitrogenase-like sequences amongst microbial genomes. *BMC Genomics*, 13(1), 162. [https://doi.org/10.1186/1471-](https://doi.org/10.1186/1471-2164-13-162)
540 [2164-13-162](https://doi.org/10.1186/1471-2164-13-162)
- 541 Dyhrman, S. T., Chappell, P. D., Haley, S. T., Moffett, J. W., Orchard, E. D., Waterbury, J. B., & Webb, E. A. (2006).
542 Phosphonate utilization by the globally important marine diazotroph *Trichodesmium*. *Nature*, 439(7072), 68–71.
543 <https://doi.org/10.1038/nature04203>
- 544 Falkowski, P. G. (1997). Evolution of the nitrogen cycle and its influence on the biological sequestration of CO₂ in the
545 ocean. *Nature*, 387(6630), 272–275. <https://doi.org/10.1038/387272a0>
- 546 Fernández-Gómez, B., Richter M, Schüller M, Pinhassi, J., Acinas, S., González, J., & Pedrós-Alió, C. (2013). Ecology of
547 marine Bacteroidetes: a comparative genomics approach. *The ISME Journal*, 7(5), 1026–1037.
548 <https://doi.org/10.1038/ismej.2012.169>
- 549 Fernández, A., Mouriño-Carballido, B., Bode, A., Varela, M., & Marañón, E. (2010). Latitudinal distribution of
550 *Trichodesmium* spp. and N₂ fixation in the Atlantic Ocean. *Biogeosciences Discussions*, 7(2), 2195–2225.
551 <https://doi.org/10.5194/bgd-7-2195-2010>
- 552 Fernández I, C., Raimbault, P., Garcia, N., & Rimmelin, P. (2005). An estimation of annual new production and carbon
553 fluxes in the northeast Atlantic Ocean during 2001. *Journal of Geophysical Research*, 110(C7), 1–15.
554 <https://doi.org/10.1029/2004JC002616>
- 555 Fiúza, A.F.G. (1984). Hidrologia e dinâmica das águas costeiras de Portugal (Hydrology and dynamics of the Portuguese
556 coastal waters). Ph.D. dissertation, Universidade de Lisboa, 294 pp.
- 557 Fonseca-Batista, D., Dehairs, F., Riou, V., Fripiat, F., Elskens, M., Deman, F., ... Auel, H. (2017). Nitrogen fixation in
558 the eastern Atlantic reaches similar levels in the Southern and Northern Hemisphere. *Journal of Geophysical Research:*
559 *Oceans*, 122, 4618–4632. <https://doi.org/10.1002/2016JC011775>.Received
- 560 Frouin, R., Fiúza, A. F. G., Ambar, I., & Boyd, T. J. (1990). Observations of a poleward surface current off the coasts of
561 Portugal and Spain during winter. *Journal of Geophysical Research*, 95(C1), 679.
562 <https://doi.org/10.1029/JC095iC01p00679>



- 563 García-Ibáñez, M. I., Pardo, P. C., Carracedo, L. I., Mercier, H., Lherminier, P., Ríos, A. F., & Pérez, F. F. (2015).
564 Structure, transports and transformations of the water masses in the Atlantic Subpolar Gyre. *Progress in Oceanography*,
565 135, 18–36. <https://doi.org/10.1016/j.pocean.2015.03.009>
- 566 Garcia, H. E., Locarnini, R. A., Boyer, T. P., Antonov, J. I., Baranova, O. K., Zweng, M. M., ... Johnson, D. R. (2013).
567 World Ocean Atlas 2013, Volume 4 : Dissolved Inorganic Nutrients (phosphate, nitrate, silicate). NOAA Atlas NESDIS
568 76 (Vol. 4). Silver Spring, Maryland, USA.
- 569 Gotelli, N. J., & Colwell, R. K. (2001). Quantifying biodiversity: procedures and pitfalls in the measurement and
570 comparison of species richness. *Ecology Letters*, 4(4), 379–391. <https://doi.org/10.1046/j.1461-0248.2001.00230.x>
- 571 Grasshoff, K., Ehrhardt, M., & Kremling, K. (1983). *Methods of Seawater Analysis*. Second, Revised and Extended
572 Edition. Verlag Chemie GmbH, D-6940 Weinheim, Germany.
- 573 Großkopf, T., Mohr, W., Baustian, T., Schunck, H., Gill, D., Kuypers, M. M. M., ... LaRoche, J. (2012). Doubling of
574 marine dinitrogen-fixation rates based on direct measurements. *Nature*, 488(7411), 361–364.
575 <https://doi.org/10.1038/nature11338>
- 576 Gruber, N. (2008). The Marine Nitrogen Cycle: Overview and Challenges. *Nitrogen in the Marine Environment*.
577 <https://doi.org/10.1016/B978-0-12-372522-6.00001-3>
- 578 Halm, H., Lam, P., Ferdelman, T. G., Lavik, G., Dittmar, T., LaRoche, J., ... Kuypers, M. M. M. (2012). Heterotrophic
579 organisms dominate nitrogen fixation in the South Pacific Gyre. *The ISME Journal*, 6(6), 1238–49.
580 <https://doi.org/10.1038/ismej.2011.182>
- 581 Hama, T., Miyazaki, T., Ogawa, Y., Iwakuma, T., Takahashi, M., Otsuki, A., & Ichimura, S. (1983). Measurement of
582 photosynthetic production of a marine phytoplankton population using a stable ¹³C isotope. *Marine Biology*, 73, 31–
583 36.
- 584 Holmes, R. M., Aminot, A., Kérouel, R., Hooker, B. A., & Peterson, B. J. (1999). A simple and precise method for
585 measuring ammonium in marine and freshwater ecosystems. *Canadian Journal of Fisheries and Aquatic Sciences*,
586 56(10), 1801–1808. <https://doi.org/10.1139/f99-128>
- 587 Hongoh, Y., Sharma, V. K., Prakash, T., Noda, S., Toh, H., Taylor, T. D., ... Ohkuma, M. (2008). Genome of an
588 endosymbiont coupling N₂ fixation to cellulolysis within protist cells in termite gut. *Science (New York, N.Y.)*,
589 322(5904), 1108–9. <https://doi.org/10.1126/science.1165578>
- 590 Howard, J. B., & Rees, D. C. (1996). Structural Basis of Biological Nitrogen Fixation. *Chemical Reviews*, 96(7), 2965–
591 2982. <https://doi.org/10.1021/cr9500545>
- 592 Inoue, J., Oshima, K., Suda, W., Sakamoto, M., Iino, T., Noda, S., ... Ohkuma, M. (2015). Distribution and evolution of
593 nitrogen fixation genes in the phylum Bacteroidetes. *Microbes and Environments / JSME*, 30(1), 44–50.
594 <https://doi.org/10.1264/jsme2.ME14142>
- 595 Jickells, T. D. (1999). The inputs of dust derived elements to the Sargasso Sea; a synthesis. *Marine Chemistry*, 68(1–2),
596 5–14. [https://doi.org/10.1016/S0304-4203\(99\)00061-4](https://doi.org/10.1016/S0304-4203(99)00061-4)
- 597 Krupke, A., Lavik, G., Halm, H., Fuchs, B. M., Amann, R. I., & Kuypers, M. M. M. (2014). Distribution of a consortium
598 between unicellular algae and the N₂ fixing cyanobacterium UCYN-A in the North Atlantic Ocean. *Environmental*
599 *Microbiology*, 16(10), 3153–3167. <https://doi.org/10.1111/1462-2920.12431>
- 600 Kumar, S., Stecher, G., & Tamura, K. (2016). MEGA7: Molecular Evolutionary Genetics Analysis version 7.0 for bigger
601 datasets. *Molecular Biology and Evolution*, msw054. <https://doi.org/10.1093/molbev/msw054>



- 602 Landolfi, A., Koeve, W., Dietze, H., Kähler, P., & Oschlies, A. (2015). A new perspective on environmental controls.
603 Geophysical Research Letters, 42(May), 4482–2289. <https://doi.org/10.1002/2015GL063756>.Abstract
- 604 Langlois, R. J., LaRoche, J., & Raab, P. a. (2005). Diazotrophic Diversity and Distribution in the Tropical and
605 Subtropical Atlantic Ocean Diazotrophic Diversity and Distribution in the Tropical and Subtropical Atlantic Ocean.
606 Applied and Environmental Microbiology, 71(12), 7910–7919. <https://doi.org/10.1128/AEM.71.12.7910>
- 607 Langlois, R. J., Hümmer, D., & LaRoche, J. (2008). Abundances and distributions of the dominant nifH phylotypes in the
608 Northern Atlantic Ocean. Applied and Environmental Microbiology, 74(6), 1922–1931.
609 <https://doi.org/10.1128/AEM.01720-07>
- 610 Langlois, R., Großkopf, T., Mills, M., Takeda, S., & LaRoche, J. (2015). Widespread Distribution and Expression of
611 Gamma A (UMB), an Uncultured, Diazotrophic, γ -Proteobacterial nifH Phylotype. PloS One, 10(6), e0128912.
612 <https://doi.org/10.1371/journal.pone.0128912>
- 613 Lemaitre, N., Planchon, F., Planquette, H., Dehairs, F., Fonseca-Batista, D., Roukaerts, A., Deman, F., Mariez, C., Tang,
614 Y., Sarthou, G. High variability of export fluxes along the North Atlantic GEOTRACES section GA01 – Part I:
615 Particulate organic carbon export deduced from the ^{234}Th method. Submitted to this Biogeosciences Special Issue
- 616 Li, X., Fonseca-Batista, D., Roevros N., Dehairs, F., Chou, L. Environmental and nutrient controls of marine nitrogen
617 fixation. Under Review for Progress in Oceanography
- 618 Loescher, C. R., Großkopf, T., Desai, F. D., Gill, D., Schunck, H., Croot, P. L., ... Schmitz, R. A. (2014). Facets of
619 diazotrophy in the oxygen minimum zone waters off Peru. ISME Journal, 8(11), 2180–2192.
620 <https://doi.org/10.1038/ismej.2014.71>
- 621 Luo, Y.-W., Doney, S. C., Anderson, L. A., Benavides, M., Berman-Frank, I., Bode, A., ... Zehr, J. P. (2012). Database
622 of diazotrophs in global ocean: abundance, biomass and nitrogen fixation rates. Earth System Science Data, 4(1), 47–
623 73. <https://doi.org/10.5194/essd-4-47-2012>
- 624 Luo, Y.-W., Lima, I. D., Karl, D. M., Deutsch, C. A., & Doney, S. C. (2014). Data-based assessment of environmental
625 controls on global marine nitrogen fixation. Biogeosciences, 11(3), 691–708. <https://doi.org/10.5194/bg-11-691-2014>
- 626 Man-Aharonovich, D., Kress, N., Zeev, E. B., Berman-Frank, I., & Béjà, O. (2007). Molecular ecology of nifH genes and
627 transcripts in the eastern Mediterranean Sea. Environmental Microbiology, 9(9), 2354–2363.
628 <https://doi.org/10.1111/j.1462-2920.2007.01353.x>
- 629 Marañón, E., Holligan, P. M., Varela, M., Mouriño, B., & Bale, A. J. (2000). Basin-scale variability of phytoplankton
630 biomass, production and growth in the Atlantic Ocean. Deep Sea Research Part I: Oceanographic Research Papers.
631 [https://doi.org/10.1016/S0967-0637\(99\)00087-4](https://doi.org/10.1016/S0967-0637(99)00087-4)
- 632 Martínez-Pérez, C., Mohr, W., Löscher, C. R., Dekaezemaker, J., Littmann, S., Yilmaz, P., ... Kuypers, M. M. M.
633 (2016). The small unicellular diazotrophic symbiont, UCYN-A, is a key player in the marine nitrogen cycle. Nature
634 Microbiology, 1(September), 1–7. <https://doi.org/10.1038/nmicrobiol.2016.163>
- 635 McCartney, M. S., & Talley, L. D. (1982). The Subpolar Mode Water of the North Atlantic Ocean. Journal of Physical
636 Oceanography. [https://doi.org/10.1175/1520-0485\(1982\)012<1169:TSMWOT>2.0.CO;2](https://doi.org/10.1175/1520-0485(1982)012<1169:TSMWOT>2.0.CO;2)
- 637 Mills, M. M., Ridame, C., Davey, M., La Roche, J., & Geider, R. J. (2004). Iron and phosphorus co-limit nitrogen
638 fixation in the eastern tropical North Atlantic. Nature, 429(May), 292–294. <https://doi.org/10.1038/nature02550>
- 639 Mohr, W., Großkopf, T., Wallace, D. W. R., & LaRoche, J. (2010). Methodological underestimation of oceanic nitrogen
640 fixation rates. PLoS ONE, 5(9), 1–7. <https://doi.org/10.1371/journal.pone.0012583>



- 641 Montoya, J. P., Voss, M., Kahler, P., & Capone, D. G. (1996). A Simple , High-Precision , High-Sensitivity Tracer Assay
642 for N₂ Fixation. *Applied and Environmental Microbiology*, 62(3), 986–993.
- 643 Montoya, J. P., Voss, M., & Capone, D. G. (2007). Spatial variation in N₂-fixation rate and diazotroph activity in the
644 Tropical Atlantic. *Biogeosciences*, 4(3), 369–376. <https://doi.org/10.5194/bg-4-369-2007>
- 645 Moore, C. M., Mills, M. M., Achterberg, E. P., Geider, R. J., LaRoche, J., Lucas, M. I., ... Woodward, E. M. S. (2009).
646 Large-scale distribution of Atlantic nitrogen fixation controlled by iron availability. *Nature Geoscience*, 2(12), 867–
647 871. <https://doi.org/10.1038/ngeo667>
- 648 Moreira-Coello, V., Mouriño-Carballido, B., Marañón, E., Fernández-Carrera, A., Bode, A., & Varela, M. M. (2017).
649 Biological N₂ Fixation in the Upwelling Region off NW Iberia: Magnitude, Relevance, and Players. *Frontiers in*
650 *Marine Science*, 4(September). <https://doi.org/10.3389/fmars.2017.00303>
- 651 Mulholland, M. R., Bernhardt, P. W., Blanco-Garcia, J. L., Mannino, a., Hyde, K., Mondragon, E., ... Zehr, J. P. (2012).
652 Rates of dinitrogen fixation and the abundance of diazotrophs in North American coastal waters between Cape Hatteras
653 and Georges Bank. *Limnology and Oceanography*, 57(4), 1067–1083. <https://doi.org/10.4319/lo.2012.57.4.1067>
- 654 Needoba, J. A., Foster, R. A., Sakamoto, C., Zehr, J. P., & Johnson, K. S. (2007). Nitrogen fixation by unicellular
655 diazotrophic cyanobacteria in the temperate oligotrophic North Pacific Ocean. *Limnology and Oceanography*, 52(4),
656 1317–1327. <https://doi.org/10.4319/lo.2007.52.4.1317>
- 657 Nei, M. (1987). *Molecular Evolutionary Genetics*. Tempe AZ Arizona State University (Vol. 17). Columbia University
658 Press, New York, USA.
- 659 Poulton, A. J., Holligan, P. M., Hickman, A., Kim, Y. N., Adey, T. R., Stinchcombe, M. C., ... Woodward, E. M. S.
660 (2006). Phytoplankton carbon fixation, chlorophyll-biomass and diagnostic pigments in the Atlantic Ocean. *Deep-Sea*
661 *Research Part II: Topical Studies in Oceanography*, 53(14–16), 1593–1610. <https://doi.org/10.1016/j.dsr2.2006.05.007>
- 662 Rahav, E., Bar-Zeev, E., Ohayon, S., Elifantz, H., Belkin, N., Herut, B., ... Berman-Frank, I. (2013). Dinitrogen fixation
663 in aphotic oxygenated marine environments. *Frontiers in Microbiology*, 4(AUG), 1–11.
664 <https://doi.org/10.3389/fmicb.2013.00227>
- 665 Rahav, E., Giannetto, M. J., & Bar-Zeev, E. (2016). Contribution of mono and polysaccharides to heterotrophic N₂
666 fixation at the eastern Mediterranean coastline. *Scientific Reports*, 6(May), 1–11. <https://doi.org/10.1038/srep27858>
- 667 Ras, J., Claustre, H., & Uitz, J. (2008). Spatial variability of phytoplankton pigment distributions in the Subtropical South
668 Pacific Ocean: comparison between in situ and predicted data. *Biogeosciences*, 5, 353–369. <https://doi.org/10.5194/bg-4-3409-2007>
- 670 Ratten, J. M., LaRoche, J., Desai, D. K., Shelley, R. U., Landing, W. M., Boyle, E., ... Langlois, R. J. (2015). Sources of
671 iron and phosphate affect the distribution of diazotrophs in the North Atlantic. *Deep-Sea Research Part II: Topical*
672 *Studies in Oceanography*, 116, 332–341. <https://doi.org/10.1016/j.dsr2.2014.11.012>
- 673 Raven, J. A. (1988). The iron and molybdenum use efficiencies of plant growth with different energy, carbon and
674 nitrogen sources. *New Phytologist*, 109, 279–287. <https://doi.org/10.1111/j.1469-8137.1988.tb04196.x>
- 675 Rees, A., Gilbert, J., & Kelly-Gerreyn, B. (2009). Nitrogen fixation in the western English Channel (NE Atlantic Ocean).
676 *Marine Ecology Progress Series*, 374(1979), 7–12. <https://doi.org/10.3354/meps07771>
- 677 Rijkenberg, M. J. A., Langlois, R. J., Mills, M. M., Patey, M. D., Hill, P. G., Nielsdóttir, M. C., ... Achterberg, E. P.
678 (2011). Environmental forcing of nitrogen fixation in the Eastern Tropical and Sub-Tropical North Atlantic Ocean.
679 *PLoS ONE*, 6(12). <https://doi.org/10.1371/journal.pone.0028989>



- 680 Riou, V., Fonseca-Batista, D., Roukaerts, A., Biegala, I. C., Prakya, S. R., Magalhães Loureiro, C., ... Dehairs, F. (2016).
681 Importance of N₂-Fixation on the Productivity at the North-Western Azores Current/Front System, and the Abundance
682 of Diazotrophic Unicellular Cyanobacteria. *Plos One*, 11(3), e0150827. <https://doi.org/10.1371/journal.pone.0150827>
- 683 Rivero-Calle, S., Castillo, C. E. Del, Gnanadesikan, A., Dezfuli, A., Zaitchik, B., & Johns, D. G. (2016). Interdecadal
684 *Trichodesmium* variability in cold North Atlantic waters. *Global Biogeochemical Cycles*, 30, 1–19.
685 <https://doi.org/10.1002/2015GB005326>.Received
- 686 Sarthou, G., Baker, A. R., Blain, S., Achterberg, E. P., Boye, M., Bowie, A. R., ... Worsfold, P. J. (2003). Atmospheric
687 iron deposition and sea-surface dissolved iron concentrations in the eastern Atlantic Ocean. *Deep-Sea Research Part I: Oceanographic Research Papers*, 50(10–11), 1339–1352. [https://doi.org/10.1016/S0967-0637\(03\)00126-2](https://doi.org/10.1016/S0967-0637(03)00126-2)
- 688 Scavotto, R. E., Dziallas, C., Bentzon-Tilia, M., Riemann, L., & Moisander, P. H. (2015). Nitrogen-fixing bacteria
689 associated with copepods in coastal waters of the North Atlantic Ocean. *Environmental Microbiology*, 17(10), 3754–
690 3765. <https://doi.org/10.1111/1462-2920.12777>
- 692 Shelley, R. U., Roca-Martí, M., Castrillejo, M., Masqué, P., Landing, W. M., Planquette, H., & Sarthou, G. (2017).
693 Quantification of trace element atmospheric deposition fluxes to the Atlantic Ocean (>40°N; GEOVIDE, GEOTRACES
694 GA01) during spring 2014. *Deep-Sea Research Part I: Oceanographic Research Papers*, 119(November 2016), 34–49.
695 <https://doi.org/10.1016/j.dsr.2016.11.010>
- 696 Shiozaki, T., Kodama, T., Kitajima, S., Sato, M., & Furuya, K. (2013). Advective transport of diazotrophs and
697 importance of their nitrogen fixation on new and primary production in the western Pacific warm pool. *Limnology and
698 Oceanography*, 58(1), 49–60. <https://doi.org/10.4319/lo.2013.58.1.0049>
- 699 Shiozaki, T., Ijichi, M., Kodama, T., Takeda, S., Furuya, K., Ijichi, M., ... Furuya, K. (2014). Heterotrophic bacteria as
700 major nitrogen fixers in the euphotic zone of the Indian Ocean. *Global Biogeochemical Cycles*, 28, 1096–1110.
701 <https://doi.org/10.1002/2014GB004886>.Received
- 702 Shiozaki, T., Nagata, T., Ijichi, M., & Furuya, K. (2015). Nitrogen fixation and the diazotroph community in the
703 temperate coastal region of the northwestern North Pacific. *Biogeosciences*, 12(15), 4751–4764.
704 <https://doi.org/10.5194/bg-12-4751-2015>
- 705 Snow, J. T., Schlosser, C., Woodward, E. M. S., Mills, M. M., Achterberg, E. P., Mahaffey, C., ... Moore, C. M. (2015).
706 Environmental controls on the biogeography of diazotrophy and *Trichodesmium* in the Atlantic Ocean. *Global
707 Biogeochemical Cycles*, 29, 865–884. <https://doi.org/10.1002/2013GB004679>.Received
- 708 Sohm, J. A., & Capone, D. G. (2006). Phosphorus dynamics of the tropical and subtropical north Atlantic:
709 *Trichodesmium* spp. versus bulk plankton. *Marine Ecology Progress Series*, 317, 21–28.
710 <https://doi.org/10.3354/meps317021>
- 711 Sohm, J. A., Webb, E. A., & Capone, D. G. (2011). Emerging patterns of marine nitrogen fixation. *Nature Reviews.
712 Microbiology*, 9(7), 499–508. <https://doi.org/10.1038/nrmicro2594>
- 713 Subramaniam, A., Yager, P. L., Carpenter, E. J., Mahaffey, C., Björkman, K., Cooley, S., ... Capone, D. G. (2008).
714 Amazon River enhances diazotrophy and carbon sequestration in the tropical North Atlantic Ocean. *Global
715 Biogeochemical Cycles*, 105, 10460–10465. <https://doi.org/10.1029/2006GB002751>
- 716 Subramaniam, A., Mahaffey, C., Johns, W., & Mahowald, N. (2013). Equatorial upwelling enhances nitrogen fixation in
717 the Atlantic Ocean. *Geophysical Research Letters*, 40(9), 1766–1771. <https://doi.org/10.1002/grl.50250>



- 718 Swan, C. M., Vogt, M., Gruber, N., & Laufkoetter, C. (2016). A global seasonal surface ocean climatology of
719 phytoplankton types based on CHEMTAX analysis of HPLC pigments. *Deep-Sea Research Part I: Oceanographic*
720 *Research Papers*, 109, 137–156. <https://doi.org/10.1016/j.dsr.2015.12.002>
- 721 Thompson, A. W., Foster, R. A., Krupke, A., Carter, B. J., Musat, N., Vaulot, D., ... Zehr, J. P. (2012). Unicellular
722 *Cyanobacterium* Symbiotic with a Single-Celled Eukaryotic Alga. *Science*, 337(September), 1546–1550.
- 723 Thompson, A., Carter, B. J., Turk-Kubo, K., Malfatti, F., Azam, F., & Zehr, J. P. (2014). Genetic diversity of the
724 unicellular nitrogen-fixing cyanobacteria UCYN-A and its prymnesiophyte host. *Environmental Microbiology*, 16(10),
725 3238–3249. <https://doi.org/10.1111/1462-2920.12490>
- 726 Thuróczy, C.-E., Gerringa, L. J. A., Klunder, M. B., Middag, R., Laan, P., Timmermans, K. R., & de Baar, H. J. W.
727 (2010). Speciation of Fe in the Eastern North Atlantic Ocean. *Deep Sea Research Part I: Oceanographic Research*
728 *Papers*, 57(11), 1444–1453. <https://doi.org/10.1016/j.dsr.2010.08.004>
- 729 Tonnard, M., Planquette, H., Bowie, A. R., van der Merwe, P., Gallinari, M., Deprez de Gesincourt, F., ... Sarthou, G.
730 (2018). Dissolved iron in the North Atlantic Ocean and Labrador Sea along the GEOVIDE section (GEOTRACES
731 section GA01). *Biogeosciences Discussions*. <https://doi.org/10.5194/bg-2018-147>
- 732 Tonnard M., Donval A., Lampert L., Treguer P., Claustre H., Dimier C., Ras J., Bowie AR, van der Merwe, Planquette
733 HF, and Sarthou G. Phytoplankton assemblages in the North Atlantic Ocean and in the Labrador Sea along the
734 GEOVIDE section (GEOTRACES section GA01) determined by CHEMTAX analysis from of HPLC pigments data:
735 from an Assessment of the community structure, succession and potential limitation to broader implication. To be
736 submitted to this Biogeosciences Special Issue
- 737 Tripp, H. J., Bench, S. R., Turk, K. a, Foster, R. A., Desany, B. A., Niazi, F., ... Zehr, J. P. (2010). Metabolic
738 streamlining in an open-ocean nitrogen-fixing cyanobacterium. *Nature*, 464(7285), 90–94.
739 <https://doi.org/10.1038/nature08786>
- 740 Vidal, M., Duarte, C. M., & Agustí, S. (1999). Dissolved organic nitrogen and phosphorus pools and fluxes in the central
741 Atlantic Ocean. *Limnology and Oceanography*, 44(1), 106–115.
- 742 Vidal, M., Duarte, C. M., Agustí, S., Gasol, J. M., & Vaqué, D. (2003). Alkaline phosphatase activities in the central
743 Atlantic Ocean indicate large areas with phosphorus deficiency. *Marine Ecology Progress Series*, 262, 43–53.
744 <https://doi.org/10.3354/meps262043>
- 745 García-Ibáñez, M. I., Pardo, P. C., Carracedo, L. I., Mercier, H., Lherminier, P., Ríos, A. F., & Pérez, F. F. (2015).
746 Structure, transports and transformations of the water masses in the Atlantic Subpolar Gyre. *Progress in Oceanography*,
747 135, 18–36. <https://doi.org/10.1016/j.pocean.2015.03.009>
- 748 Shelley, R. U., Roca-Martí, M., Castrillejo, M., Sanial, V., Masqué, P., Landing, W. M., ... Sarthou, G. (2017).
749 Quantification of trace element atmospheric deposition fluxes to the Atlantic Ocean (> 40°N; GEOVIDE,
750 GEOTRACES GA01) during spring 2014. *Deep-Sea Research Part I*, 119(November 2016), 34–49.
751 <https://doi.org/10.1016/j.dsr.2016.11.010>
- 752 Thuróczy, C.-E., Gerringa, L. J. A., Klunder, M. B., Middag, R., Laan, P., Timmermans, K. R., & de Baar, H. J. W.
753 (2010). Speciation of Fe in the Eastern North Atlantic Ocean. *Deep Sea Research Part I: Oceanographic Research*
754 *Papers*, 57(11), 1444–1453. <https://doi.org/10.1016/j.dsr.2010.08.004>



- 755 Tonnard, M., Planquette, H., Bowie, A. R., van der Merwe, P., Gallinari, M., Deprez de Gesincourt, F., ... Sarthou, G.
756 (2018). Dissolved iron distribution in the North Atlantic Ocean and Labrador Sea along the GEOVIDE section
757 (GEOTRACES section GA01). *Biogeosciences Discussions*, (April).
- 758 Vidal, M., Duarte, C. M., & Agustí, S. (1999). Dissolved organic nitrogen and phosphorus pools and fluxes in the central
759 Atlantic Ocean. *Limnology and Oceanography*, 44(1), 106–115.
- 760 Vidal, M., Duarte, C. M., Agustí, S., Gasol, J. M., & Vaqué, D. (2003). Alkaline phosphatase activities in the central
761 Atlantic Ocean indicate large areas with phosphorus deficiency. *Marine Ecology Progress Series*, 262, 43–53.
762 <https://doi.org/10.3354/meps262043>
- 763 Villa-Alfageme, M., de Soto, F. C., Ceballos, E., Giering, S. L. C., Le Moigne, F. A. C., Henson, S., ... Sanders, R. J.
764 (2016). Geographical, seasonal, and depth variation in sinking particle speeds in the North Atlantic. *Geophysical*
765 *Research Letters*, 43, 8609–8616. <https://doi.org/10.1002/2016GL069233>. Received
- 766 Voss, M., Croot, P., Lochte, K., Mills, M., & Peeken, I. (2004). Patterns of nitrogen fixation along 10°N in the tropical
767 Atlantic. *Geophysical Research Letters*, 31(23), 1–4. <https://doi.org/10.1029/2004GL020127>
- 768 Yamamoto-Kawai, M., Carmack, E., & McLaughlin, F. (2006). Nitrogen balance and Arctic throughflow. *Nature*,
769 443(7107), 43. <https://doi.org/10.1038/443043a>
- 770 Yentsch, C. S., & Menzel, D. W. (1963). A method for the determination of phytoplankton chlorophyll and phaeophytin
771 by fluorescence. *Deep Sea Research and Oceanographic Abstracts*, 10(3), 221–231. [https://doi.org/10.1016/0011-](https://doi.org/10.1016/0011-7471(63)90358-9)
772 [7471\(63\)90358-9](https://doi.org/10.1016/0011-7471(63)90358-9)
- 773 Zani, S., Mellon, M. T., Collier, J. L., & Zehr, J. P. (2000). Expression of *nifH* genes in natural microbial assemblages in
774 Lake George, New York, detected by reverse transcriptase PCR. *Applied and Environmental Microbiology*, 66(7),
775 3119–3124. <https://doi.org/10.1128/AEM.66.7.3119-3124.2000>
- 776 Zehr, J. P., Waterbury, J. B., Turner, P. J., Montoya, J. P., Omoregie, E., Steward, G. F., ... Karl, D. M. (2001).
777 Unicellular cyanobacteria fix N₂ in the subtropical North Pacific Ocean. *Nature*, 412(6847), 635–638.
778 <https://doi.org/10.1038/35088063>
- 779 Zehr, J. P., Bench, S. R., Carter, B. J., Hewson, I., Niazi, F., Shi, T., ... Affourtit, J. P. (2008). Globally Distributed
780 Uncultivated Oceanic N₂-Fixing Cyanobacteria Lack Oxygenic Photosystem II. *Science*, 322(November), 1110–1112.
781 <https://doi.org/10.1126/science.1165340>
- 782 Zehr, J. P. (2011). Nitrogen fixation by marine cyanobacteria. *Trends in Microbiology*, 19(4), 162–173.
783 <https://doi.org/10.1016/j.tim.2010.12.004>
- 784

785 **Tables**

786

787

788

Table 1: Relative contribution (%) of N₂ fixation to Primary Production (PP).

Province	Station	Latitude (° N)	N ₂ fixation contribution to PP (%) (Redfield 6.6 ratio)	SD	N ₂ fixation contribution to PP (%) (mean POC/PN ratio of 6.3 ± 1.1)	SD
ENACW _{sp}	Bel-3	46.5	0	-	0	-
	Bel-5	45.3	0	-	0	-
	Bel-7	44.6	2	0.4	1	0.4
	Geo-21	46.5	1	0.02	1	0.0
ENACW _{st}	Bel-9	42.4	1	0.1	1	0.1
	Bel-11	40.7	28	1.9	25	1.8
	Bel-13	38.8	25	1.3	23	1.2
	Geo-1	40.3	3	0.2	3	0.1
	Geo-2	40.3	3	0.1	3	0.1
	Geo-13	41.4	3	0.1	3	0.1

789



790

791 **Table 2:** Principal component matrix illustrating the components (or axis) loadings, in other words the correlation of each variable to a determined axis as obtained with
 792 the XLSTAT software. The percentage of variability of the system explained by each of the two axes is indicated, for a total explained variance of 68%.

	Axis 1	Axis 2
% Variability explained:	48%	20%
Variables		
Euphotic layer integrated primary production	-0.812	0.088
Euphotic layer averaged temperature	0.942	0.130
Euphotic layer integrated Chl <i>a</i>	-0.768	-0.085
Euphotic layer integrated [NH ₄ ⁺]	-0.936	-0.007
Euphotic layer integrated [NO ₃ ⁻ + NO ₂]	-0.783	0.154
Climatological surface P* (20 m)	-0.305	0.584
Euphotic layer averaged salinity	0.125	0.943
Dry + wet dust deposition (April 2014)	0.583	-0.423
Euphotic layer integrated N₂ fixation	0.506	0.602

793



Figure legendsBG

795 **Figure 1:** Location of sampling stations during the Belgica BG2014/14 (black labels) and GEOVIDE (white labels) cruises
(May 2014) superimposed on a map of the phosphate excess ($P^* = [\text{PO}_4^{3-}] - [\text{NO}_3^-] / 16$) at 20 m depth seasonal average
(April to June from 1955 to 2012; World Ocean Atlas 2013) (Garcia et al., 2013). Areas of dominance of the Eastern North
Atlantic Central Waters of subpolar (ENACWsp) and subtropical (ENACWst) origins are separated by a blue dashed line.
Black dashed and solid contour lines illustrate 500 m and 1500 m isobaths, respectively.

800

Figure 2: θ/S diagrams obtained using CTD profiles from surface layer down to the 1500 m depth during (a) the Belgica
BG2014/14 cruise (stations Bel-3, 5, 7, 11 and 13), (b) the GEOVIDE cruise (stations Geo-1, 2, 13 and 21) and (c) both
expeditions combined. Diamonds indicate the characteristics of the major water masses encountered as presented in Fiúza
(1984) and García-Ibáñez et al. (2015): Eastern North Atlantic Central Waters (ENACW) of subpolar (ENACWsp) and
805 subtropical (ENACWst) origins, Mediterranean Water (MW) and Labrador Sea Water (LSW).

Figure 3: Spatial distribution of Chl *a* (a, d), NH_4^+ (b, e) and $\text{NO}_3^- + \text{NO}_2^-$ (c, f) concentrations along the Belgica
BG2014/14 (a to c) and GEOVIDE (d to f) transects. Sampling stations, and the area of dominance of Eastern North
Atlantic Waters of subpolar (ENACWsp) and subtropical (ENACWst) are illustrated according to the latitudinal and
810 longitudinal range of each transect. Mixed layer depths (MLD, black lines connecting diamonds) was estimated using a
temperature threshold criterion of 0.2°C relative to the temperature at 10 m (de Boyer Montégut et al., 2004).

Figure 4: Spatial distribution (\pm SD) of depth-integrated primary production (duplicates in light and dark green; mmol C m^{-2}
 d^{-1}) determined during (a) the Belgica BG2014/14 and (b) GEOVIDE cruises. Error bars represent the propagated
815 measurement uncertainty of all parameters used to compute volumetric uptake rates.

Figure 5: Time series of area-averaged chlorophyll *a* concentration (mg m^{-3}) over the period between December 2013 and
December 2014 for the $0.5^\circ \times 0.5^\circ$ grid surrounding each sampled station during (a) the Belgica BG2014/14 and (b)
GEOVIDE cruises, registered by Aqua Modis satellite (Giovanni online satellite data system). Dashed box illustrated the
820 sampling period for both cruises (May 2014).

Figure 6: Relative importance of euphotic layer integrated taxa-specific pigments at the four sites sampled during the
GEOVIDE cruise according to Tonnard et al. (in preparation for this Special Issue).

825 **Figure 7:** Spatial distribution (\pm SD) of depth-integrated N_2 fixation rates (duplicates in light and dark blue; $\mu\text{mol N m}^{-2} \text{d}^{-1}$)
determined during (a) the Belgica BG2014/14 and (b) GEOVIDE cruises. Error bars represent the propagated measurement
uncertainty of all parameters used to compute volumetric uptake rates.

Figure 8: Diversity of nifH sequences recovered during the Belgica BG2014/14 cruise; only detectable at stations Bel-11
830 and Bel-13. The number of sequences per group is indicated inside the bars for a total of 103 sequences recovered (a). The
clone-based rarefaction curve (b), was produced by repeatedly re-sampling randomly among all clones and plotting the
average number of OTU represented at each step (from 1 to the maximum number of clones, 41 and 62, for stations Bel-11
and Bel-13, respectively). The flattening of the curve indicates that a reasonable number of clones have been recovered and
that only the rarest OTUs remained unsampled (Gotelli and Colwell, 2001).

835



Figure 9: Euclidian distance biplot illustrating the axis loadings corresponding to the two components as obtained from the result of PCA based on Spearman rank correlation with depth-integrated rates of N_2 fixation and primary production (PP), phosphate excess (average P^* at 20 m depth surrounding each sampled site from the April to June; World Ocean Atlas 2013 climatology between 1955 to 2012) (Garcia et al., 2013), average dust dry + wet deposition derived during April 2014
840 satellite data (Giovanni online data system, NASA Goddard Earth Sciences Data and Information Services Center) and ambient variables (temperature, salinity, and nutrient data). Coloured dots represent the projection of each station corresponding to their biogeochemical characteristics.

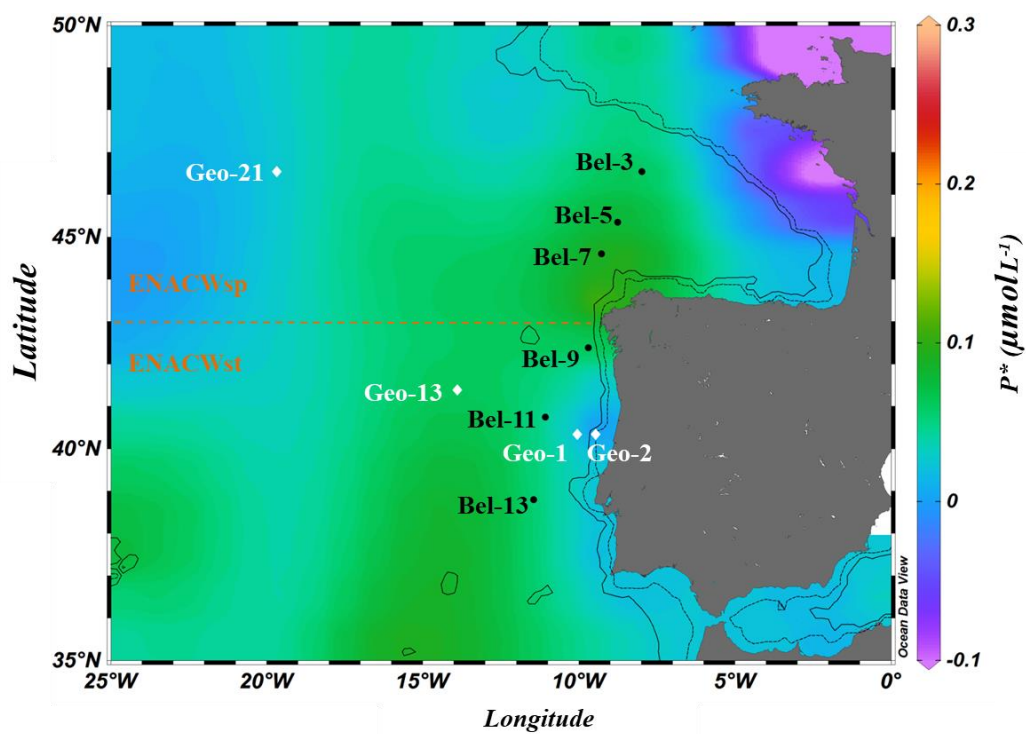


Figure 1

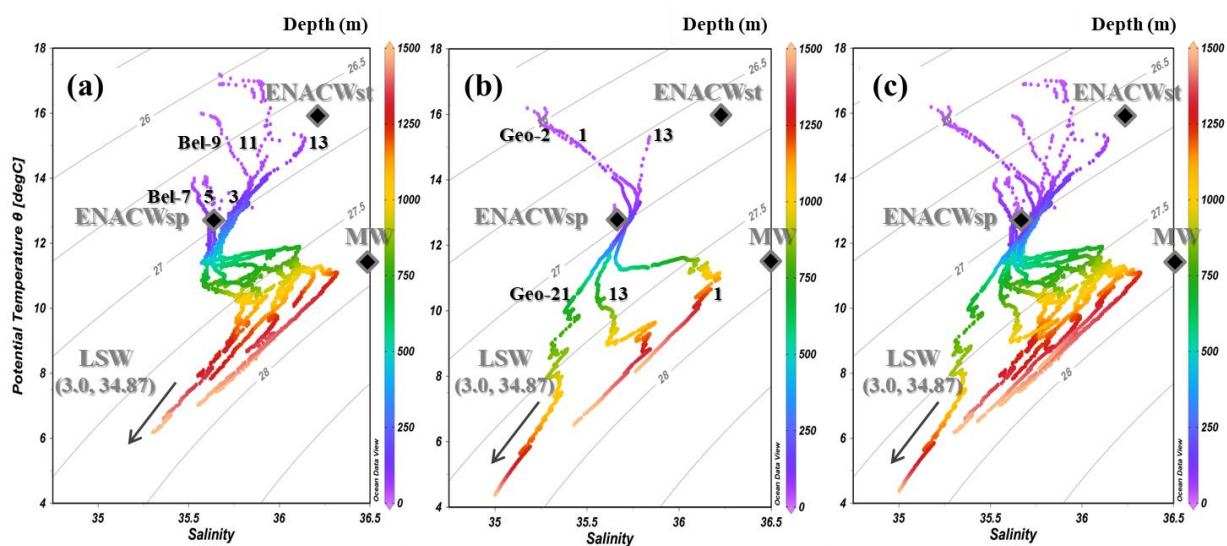


Figure 2

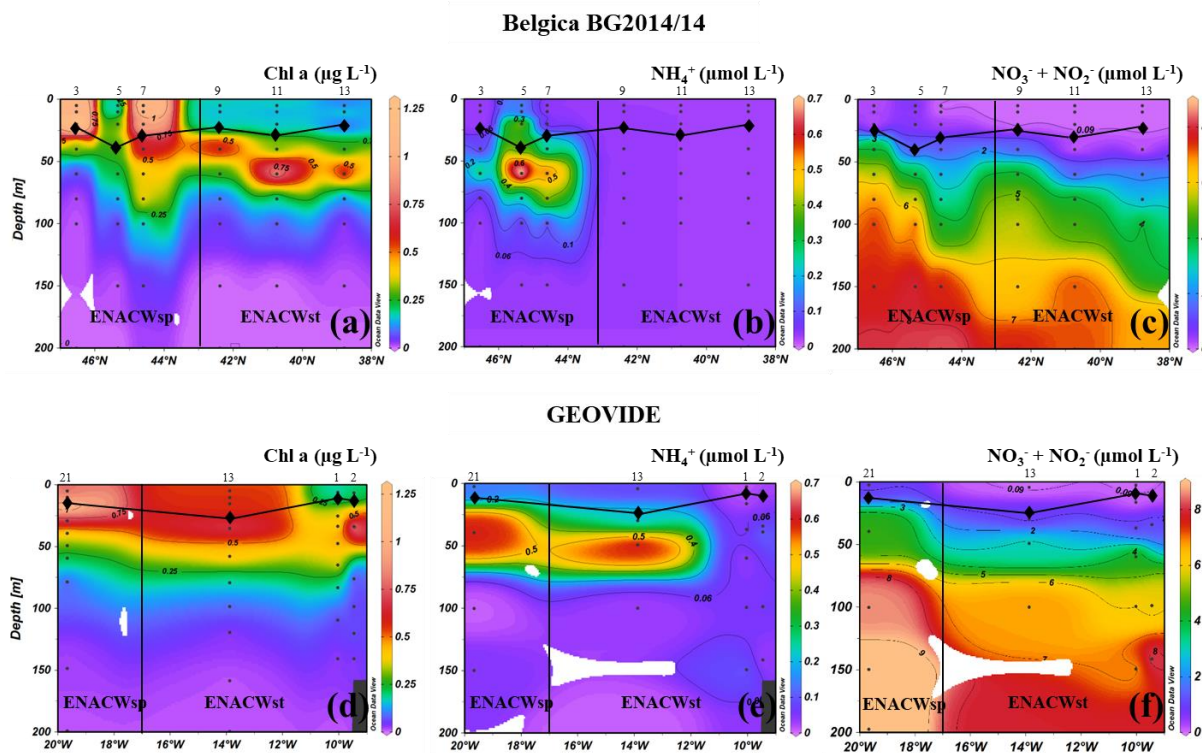


Figure 3

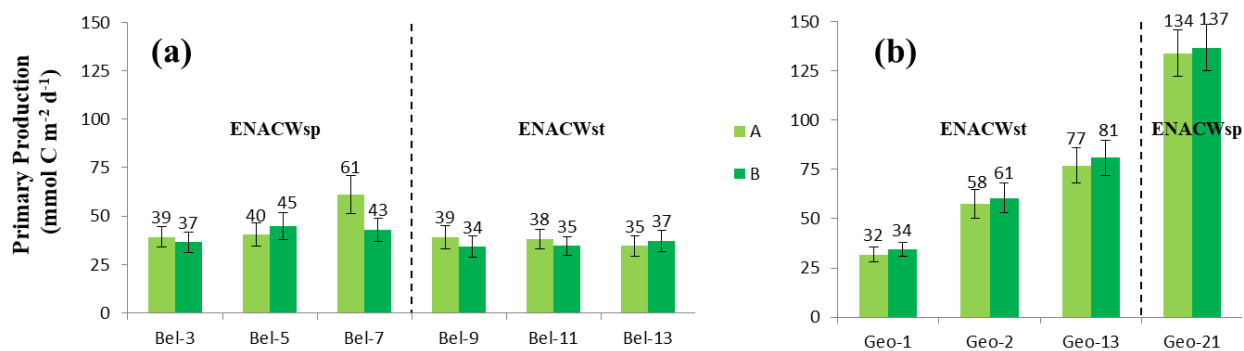


Figure 4

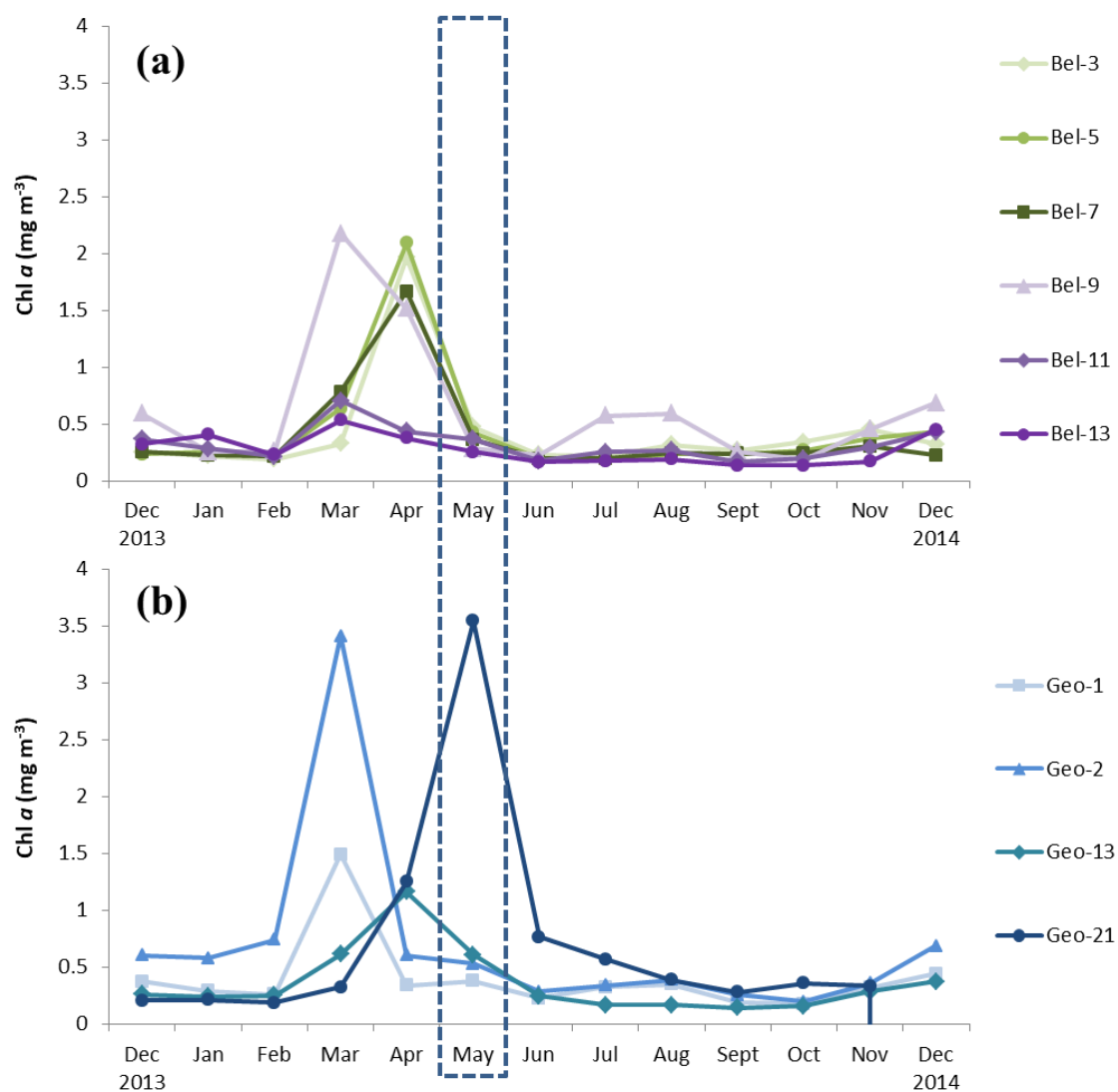


Figure 5

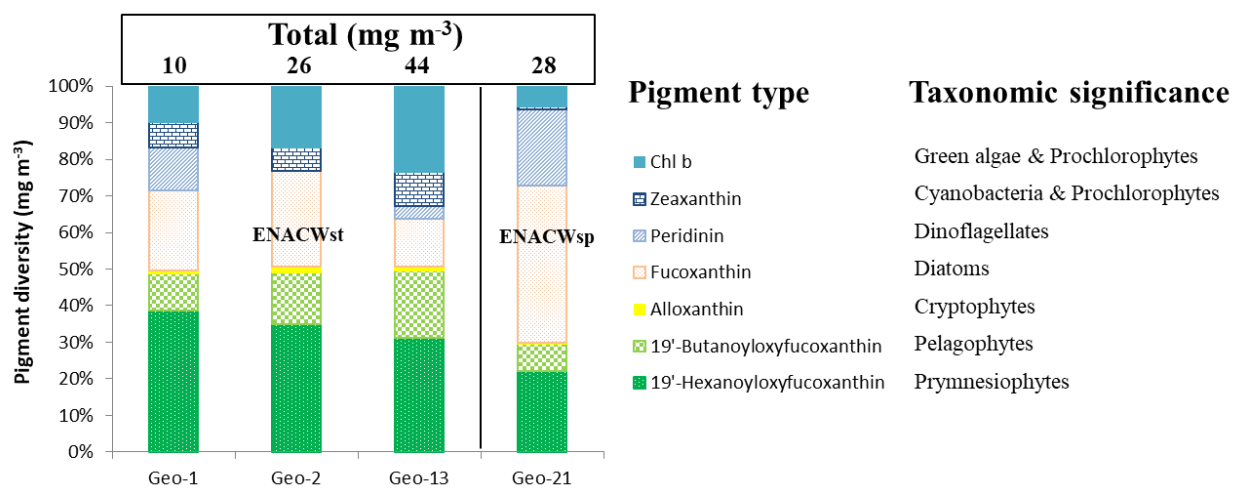


Figure 6

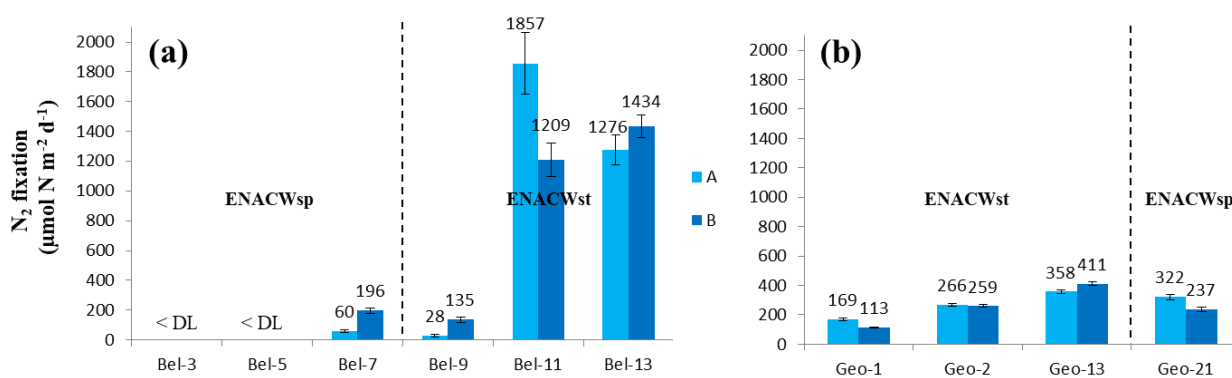


Figure 7

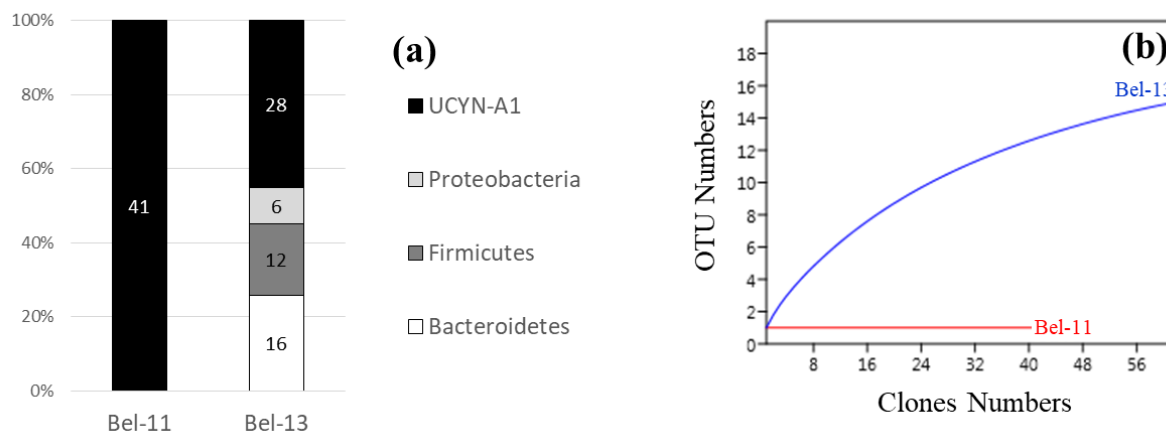


Figure 8

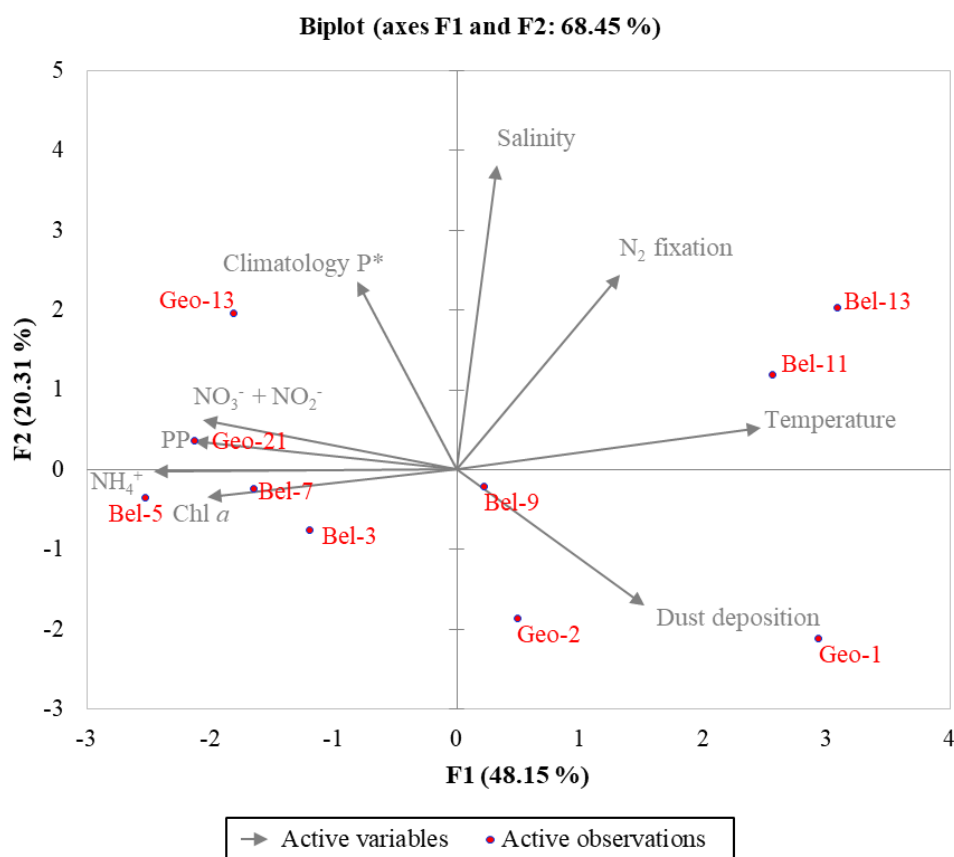


Figure 9